Quantum Sensing for Particle Physics: the NAMASSTE R&D Project

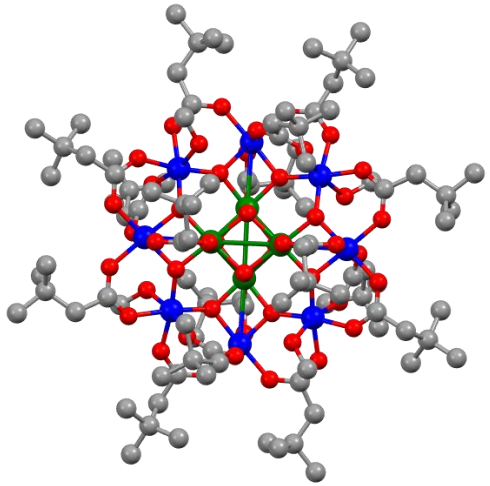

Giuseppe Latino

(Firenze University & INFN)

(on behalf of the NAMASSTE Group)

QTA&AI Workshop 2026

Siena – February 26th, 2026

Overview

- General principles of quantum sensing

- Quantum sensing in particle physics

- The INFN NAMASSTE R&D Project: motivations & results

- Summary & Conclusions

What "Quantum Sensing" Means?

"Quantum sensing" describes the use of a quantum systems, properties or phenomena to perform a measurement of a physical quantity.
Given quantum sensors (QSs) register a change of quantum state caused by the interaction with an "external system" their sensing capabilities are related to our ability to manipulate and/or read out their quantum states [1,2].

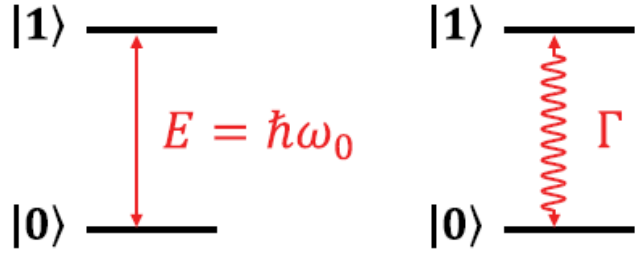

FIG. 1. Basic features of a two-state quantum system. $|0\rangle$ is the lower energy state and $|1\rangle$ is the higher energy state. Quantum sensing exploits changes in the transition frequency ω_0 or the transition rate Γ in response to an external signal V.[1]

Involved energies very low, so QSs very sensitive to external perturbations:

- **Big potentialities as precision measuring devices: why not considering them in Particle Physics?**
- **Interdisciplinary (PP community, "Quantum" community, …) R&D efforts and projects required.**
- **Many quantum systems "on the market" to be characterized as QSs and already several proposals and ongoing experiments based on quantum sensing approaches ….**

[1] C. L. Degen *et al. Rev. Mod. Phys.* 89, 035002 (2017).
[2] S.D. Bass, M. Doser, *Nat. Rev. Phys.* 6, 329 (2024).

Quantum Sensing Basic Protocol

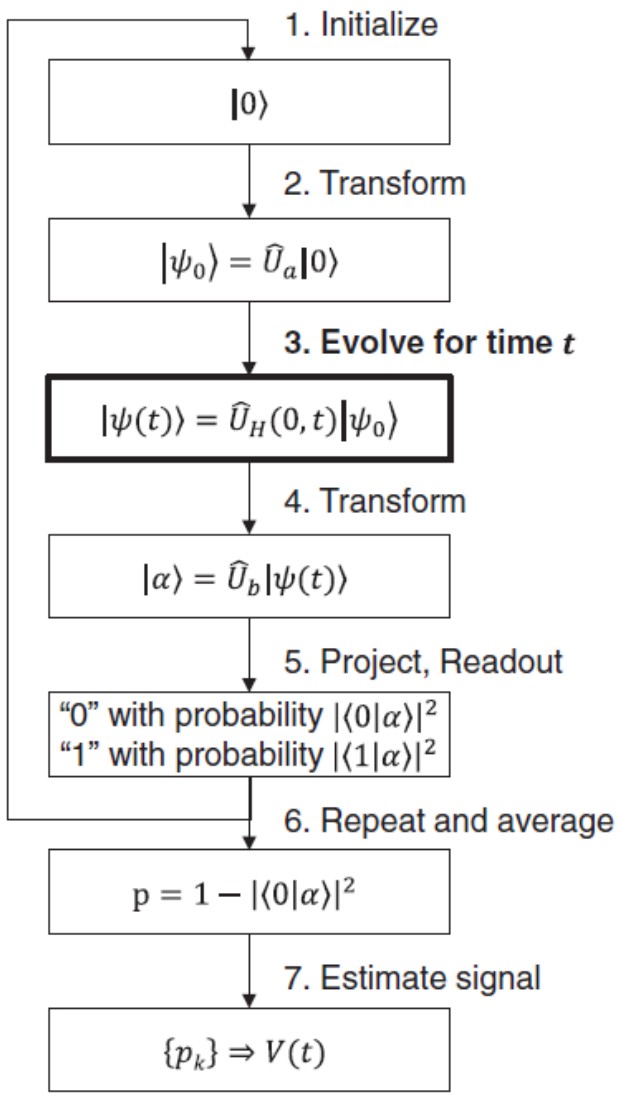

FIG. 2. Basic steps of the quantum sensing process. [1]

Quantum sensing experiments are typically performed following a basic methodology ("protocol").

In a more generic scheme the quantum sensor:

- **is initialized in a suited known state**
- **can be coherently manipulated**
- **interacts with a physical quantity (signal) for some time**
- **is read out (→ evaluation of transition probability)**
- **the physical quantity is reconstructed from the readouts (signal estimation)**

The protocol can be optimized to detect weak signals or small signal changes with the highest possible sensitivity

Quantum Sensor Hamiltonian: $\hat{H}(t) = \hat{H}_0 + \hat{H}_V(t) + \hat{H}_{\text{control}}(t)$

"Internal" H "Signal" H "Control" H

"Control" H required to manipulate the sensor either before, during or after the sensing process.

[1] Rev. Mod. Phys. 89, 035002 (2017)

A Key Example: the "Dark Side" of the Universe

Cosmological and astronomical observations: indirect evidence for BSM Physics (Dark Matter, Dark Energy)

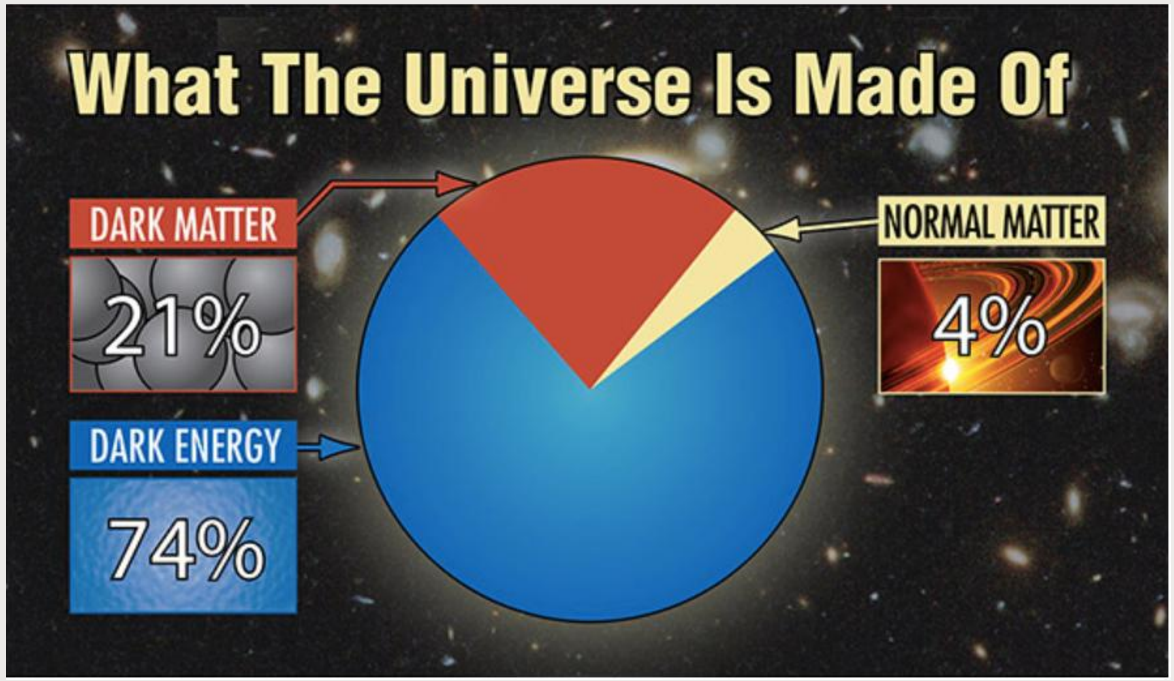

- **Several candidates theoretically +/- well motivated:** WIMPs, Axion, Dark Photon, …
- **No direct observation so far: M. Proust can be of inspiration for us …..**

  "The real voyage of discovery consists not in seeking new landscapes,

  but in having new eyes" (M. Proust, 'In Search of Lost Time' - Vol. 5)

- **Need of new detection approaches allowing to go beyond current experimental limits**
  → development of new techniques based on Quantum Sensing is a key example

Growing Interest in Quantum Technologies @ PP Facilities

Development of quantum sensing devices for fundamental physics research represents of course one the mainstream R&D activity

CERN: Quantum Technology Initiative

https://quantum.cern/

FNAL: Superconducting Quantum Materials and Systems Center

https://sqmscenter.fnal.gov/

[1] DOI: 10.17181/CERN.XDPL.W2EX

Other CERN ongoing activity: 2021 ECFA Report [1]

TF#5
Quantum & Emerging Technologies
Marcel Demarteau
Michael Doser

DRD5, aka "RDq"

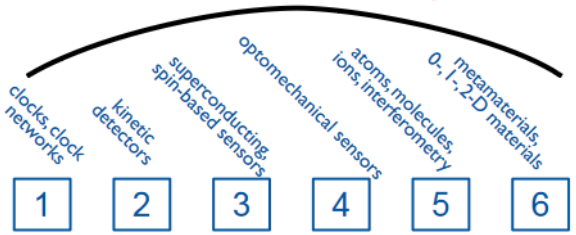

6 families identified in ECFA roadmap

DRD5 (2024)

new CERN Collaboration recently established to implement ECFA detector R&D roadmap for QS for PP

https://drd5.web.cern.ch/

An Example: Expected Improvements in Axion DM Search

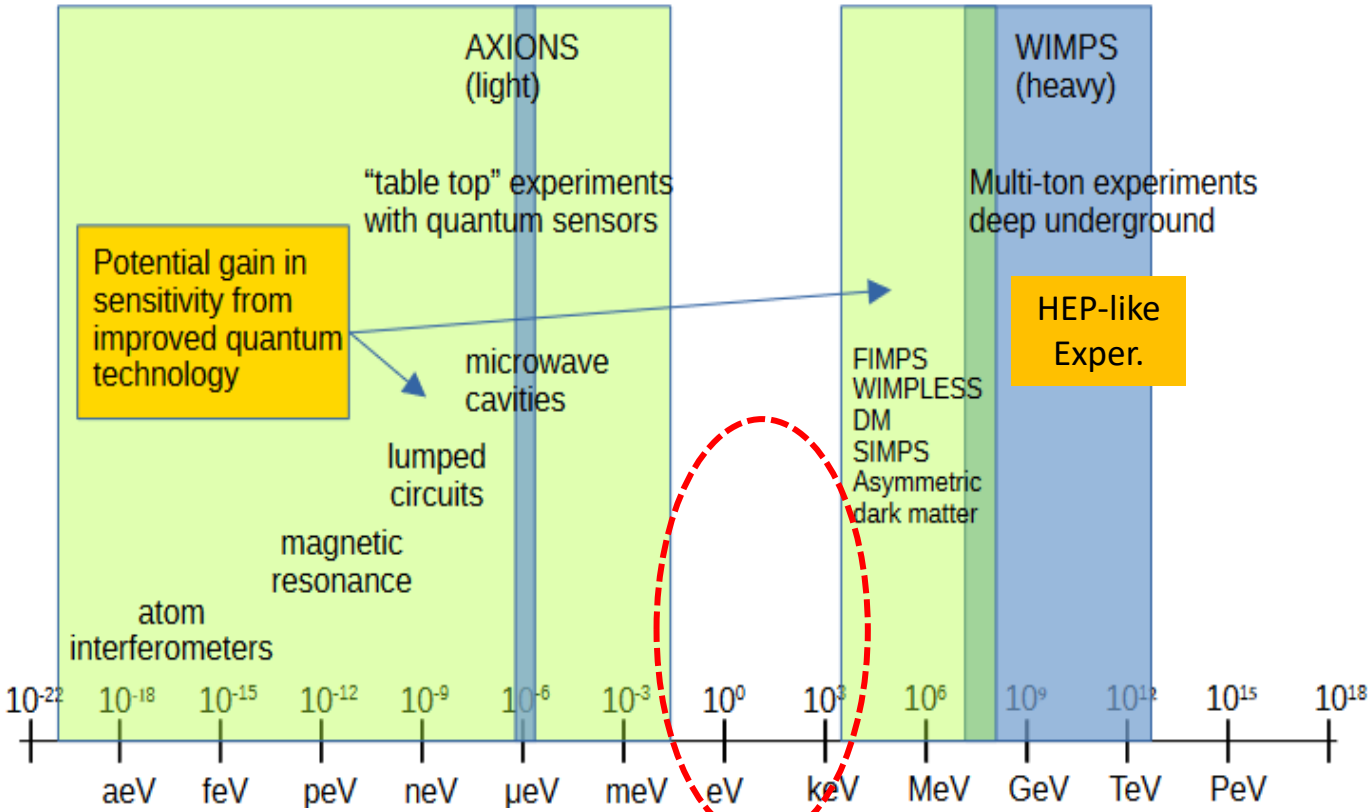

Figure 5.2: Axion mass range accessible via novel advanced quantum sensing techniques compared to current experiments. [1] (**Blue bands**: range of traditional experiments).

[1] DOI: 10.17181/CERN.XDPL.W2EX (ECFA Report)

Advantages:

- **Typically, "table-top" experiments.**
- **Require relatively limited costs/infrastructures.**
- **Relatively limited running time to reach the expected exclusion limits (big fraction of the effort in the original R&D).**

Several proposals and development of experiments already on the table:

- **CASPEr**
- **DMRadio-50L/m³**
- **QUAX**
- **……**

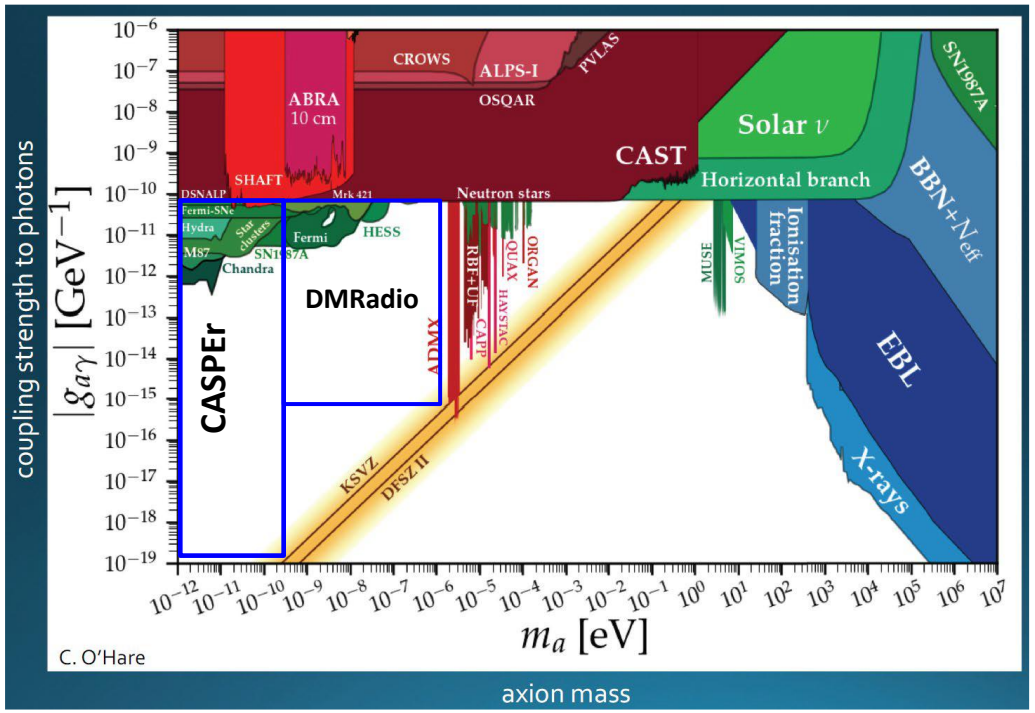

Quantum Sensors for Low Energy PP Applications

QS for low energy particle physics: the energy scale being probed is related to the one of the energy levels of the sensor itself (single interaction, typically at ≤ eV scale).

Some review papers: [1,2,3]

Physics Goals

- Search for NP/BSM (ex. α_{em} variations)
- Axions, ALP's, DM & non-DM UL-particle searches
- ν physics (masses)
- Tests of QM (ex. wavefunction collapse, decoherence)
- EDM searches, tests of fundamental symmetries

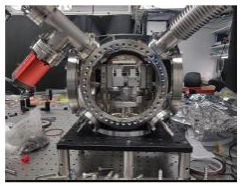

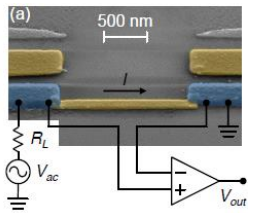

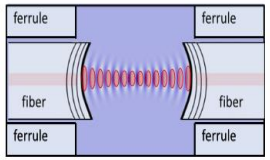

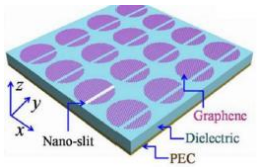

Quantum Technologies
(as identified in ECFA roadmap [4])

Clocks and clocks networks

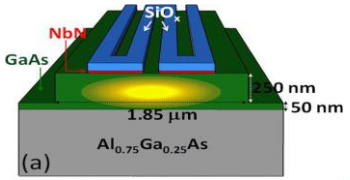

Kinetics detectors

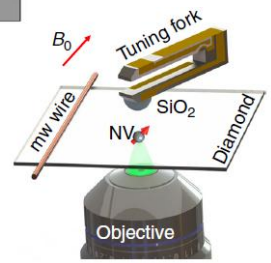

Superconducting (TES, SNSPD, …) and spin-based (NV-diamonds, SMMs, ….) devices

Optomechanical sensors

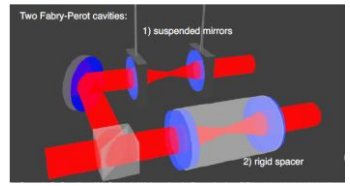

Atoms, molecules, ions, interferometry

Metamaterials, 0/1/2-D materials

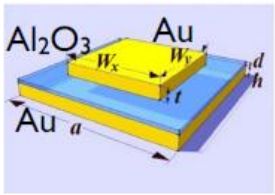

[1] DOI: 10.1038/s42254-024-00714-3
[2] DOI: 10.48550/arXiv.2311.01930
[3] DOI: 10.48550/arXiv.2311.07270
[4] DOI: 10.17181/CERN.XDPL.W2EX

Quantum Sensors for High Energy PP Applications

QS for high energy particle physics: quantum systems form part of a larger system, in which their specific properties enhance existing methods or enable novel types of detectors optimized for high energy particle physics (multiple interaction, typically at > KeV scale).

Not yet developed concepts (still speculative)

Typical Requests for Improvements in:

- **tracking (hit positions, material budget)**
- **timing (TOF for PID)**
- **calorimetry (shower shape, timing, granularity)**
- **novel observables (helicity/polarization)**

[1] DOI: 10.3389/fphy.2022.887738
[2] DOI: 10.17181/CERN.XDPL.W2EX

Applications from Quantum Technologies [1]
(as proposed in ECFA roadmap [2])

Spin-based sensors
Helicity detectors

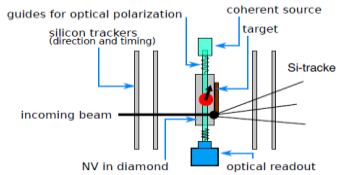

Atoms, molecules, ions
Rydberg atom TPC's

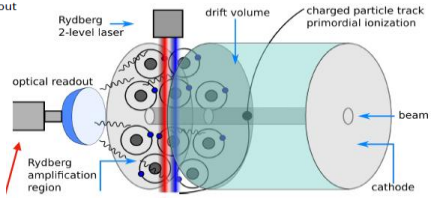

Metamaterials, 0/1/2-D materials
Ultra-fast scintillators based on perovskytes
Active scintillators (QCL, QWs, QDs)
Chromatic calorimetry (QDs)
GEMs (graphene)

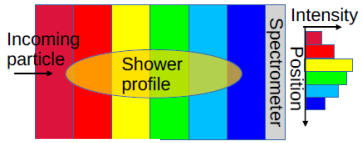

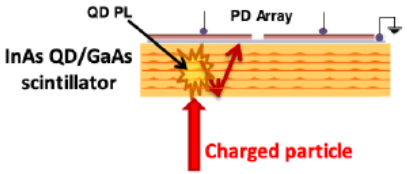

Single Molecule Magnets (SMMs)

SMMs are crystalline materials characterized by [1]:

1. Regular crystalline structure, made by identical molecules with a magnetic core of a finite number (n>1) of paramagnetic centers, with strong intramolecular exchange interactions.
2. Molecules shielded by organic ligands
   → weak intermolecular interactions.

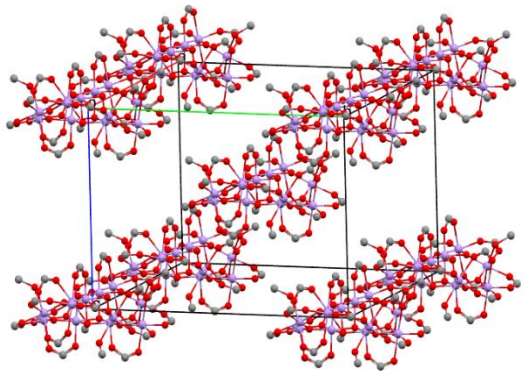

Mn_{12} crystal

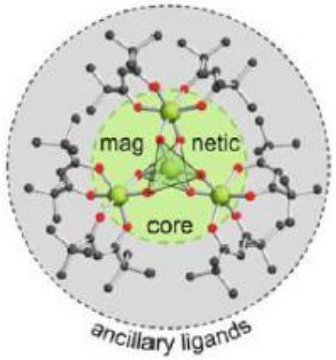

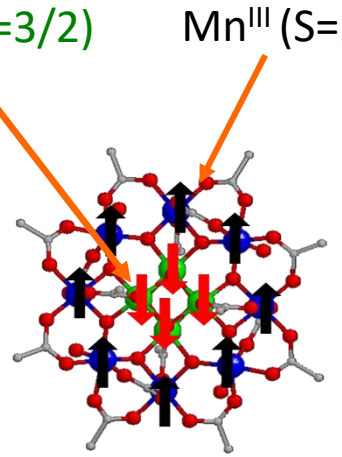

Mn_{12} core

- **Magnetically isolated molecules**
- **High spin S value** →
- **Strong uniaxial anisotropy → magnetic bi-stability at low T**
- **Quantum tunnelling of magnetization**

"Reference" (the most studied) SMM, Mn_{12}:

S_{tot}= 10; $\Delta E \approx 65$ K (~ 6 meV); $\tau \sim \tau_0 \exp(\Delta E/k_B T)$, $\tau_0 \approx 10^{-7}$s

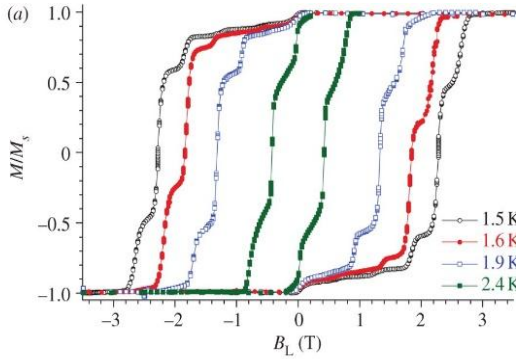

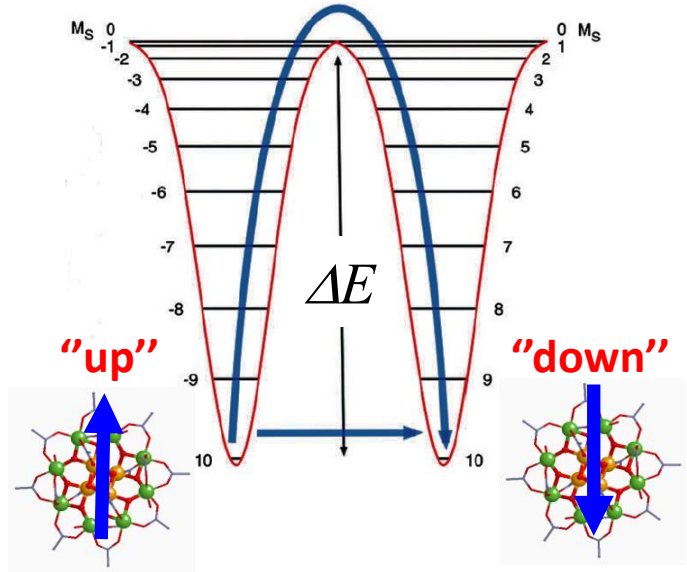

Relatively new materials with interesting potential applications …..

[1] Gatteschi, Sessoli, *Angew. Chem. Int. Ed.* **42** (2003)

Potential Applications of SMMs

High-density memory storage [1]

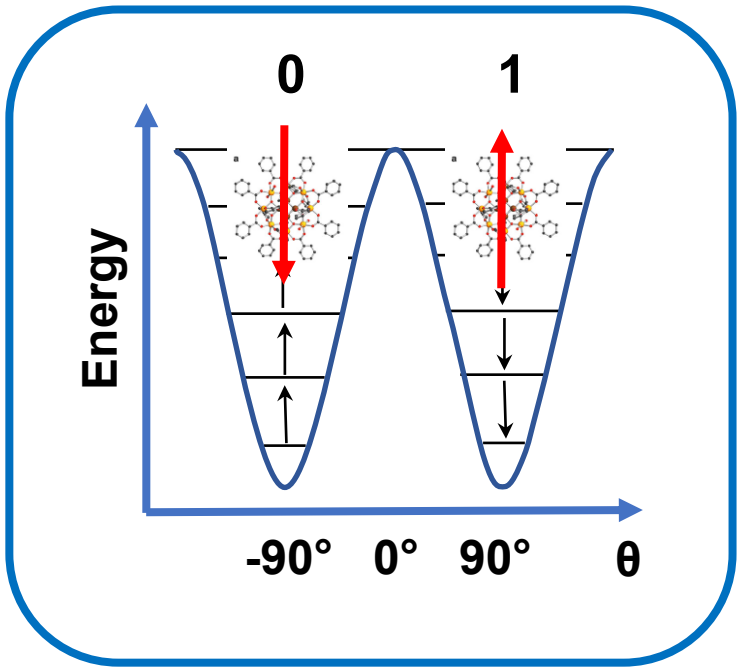

[1] Mannini *et al. Nat. Mater.* **8**, 194 (2009)

Quantum computing [2]

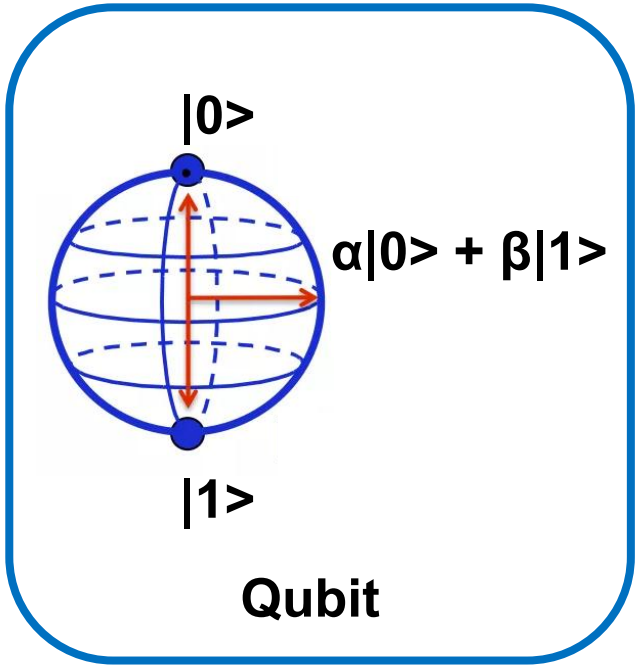

[2] Leunberger *et al. Nature* **410**, 789-793 (2001)

Molecular spintronics [3]

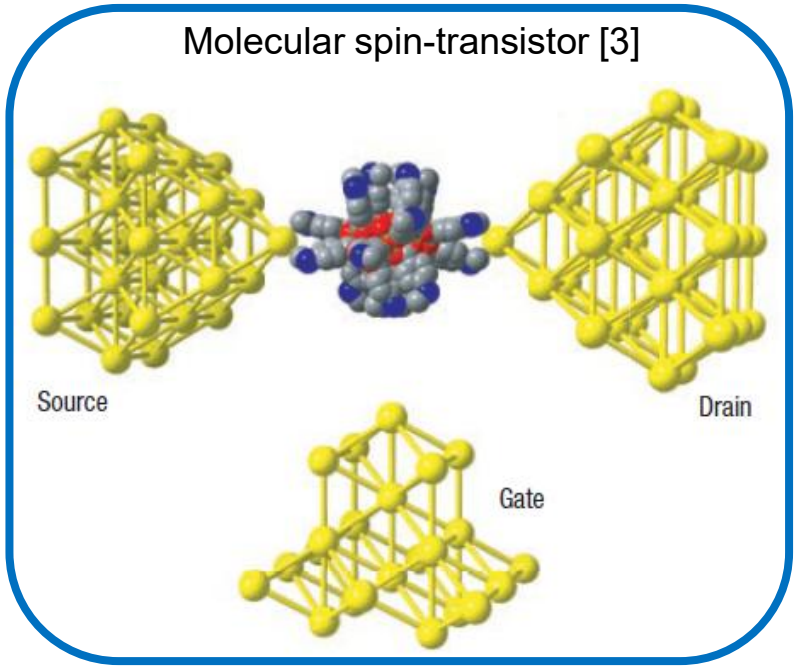

[3] Bogani *et al. Nat. Mater.* **7**, 179-186 (2008)

New potential application

Quantum sensors for particle detection → **Dedicated R&D activity required …..**

Is Mn_{12} SMM of Interest for Particle Physics ?

Bunting *et al., Phys. Rev. D* 95, 095001 (2017):

Mn_{12} SMM as sensor can detect Dark Photons at low masses, covering a region not yet experimentally explored with sensitivities exceeding current bounds

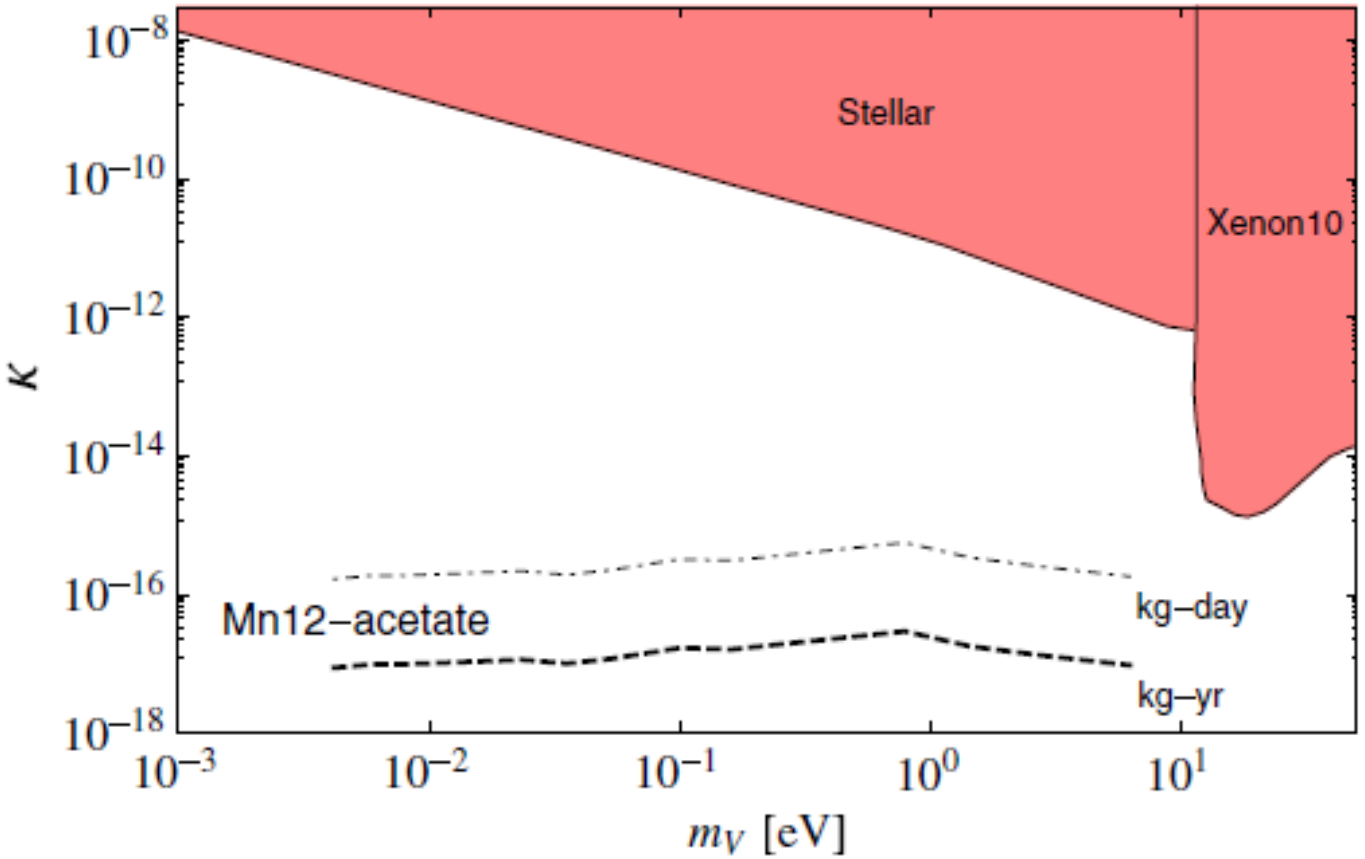

The tiny energy released by DM in the **meV-10eV** energy range could match the fine structure of the SMMs energy levels, so exciting its intramolecular vibrational modes.

$$\mathcal{L} = -\frac{1}{4}F_{\mu\nu}^2 - \frac{1}{4}V_{\mu\nu}^2 - \frac{\kappa}{2}F_{\mu\nu}V^{\mu\nu} + \frac{m_V^2}{2}V_\mu V^\mu + eJ_{\rm em}^\mu A_\mu$$

FIG. 6. Estimated sensitivity to absorption of dark vector DM in Mn_{12}-acetate, assuming an aggressive sensitivity of 1 event/kg year (dashed), and a sensitivity of 1 event/kg day (dot-dashed). The absorption data from Refs. [62,65] (described in the appendix) has been smoothed, an interpolation used in the region $m_V \sim 0.2$–0.5 eV, for which no data was available, and we use the approximation $\kappa \simeq \kappa_{\rm eff}$ (see text).

But the potential for other applications in PP has yet to be fully investigated ….

Mn_{12} SMM as Quantum Sensor

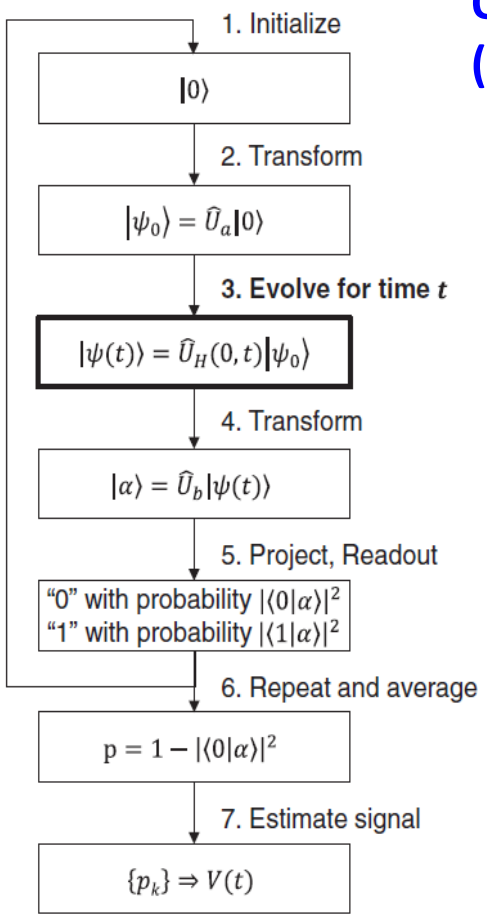

FIG. 2. Basic steps of the quantum sensing process. [1]

[1] Rev. Mod. Phys. 89, 035002 (2017)

Quantum sensing experiments are typically performed following a basic methodology ("protocol"), which requires to manipulate and/or read out the quantum states of a system.

Quantum Sensor Hamiltonian: $H(t) = H_0 + H_S(t) + H_C(t)$ ← "Control" H (required to manipulate the sensor either before, during or after the sensing process)

"Internal" H "Signal" H

Mn_{12} Spin Hamiltonian if "no signal": $H = H_0 + H_c$

$H_0 \approx - DS_z^2 - BS_z^4 + H'$ **H': contains non axial (tunnelling) terms**

$H_c = - g_z \mu_B S_z B_Z$ **Zeeman term obtained with a field B along the main crystal c-axis (easy axis)**

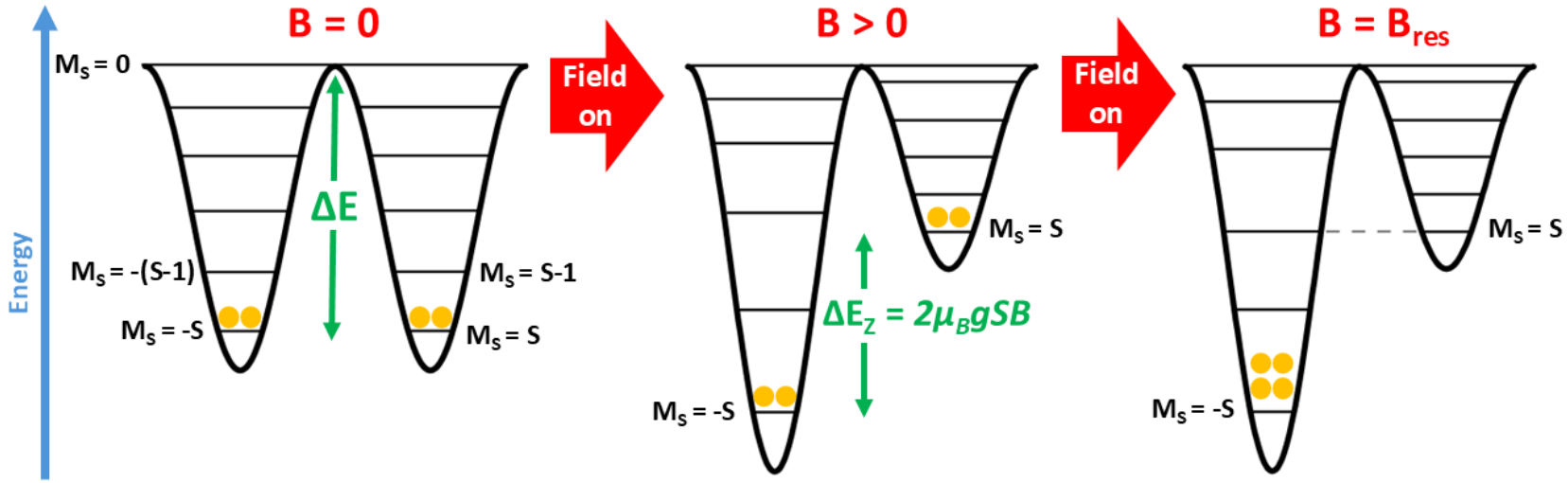

Mn_{12} SMMs as Sensors

Current detection approach [1]: an impinging particle may induce a "***magnetic avalanche***" in SMM crystals immersed in a magnetic field. This effect is triggered by the release of the Zeeman energy stored in the metastable states of the SMM in presence of an external magnetic field.

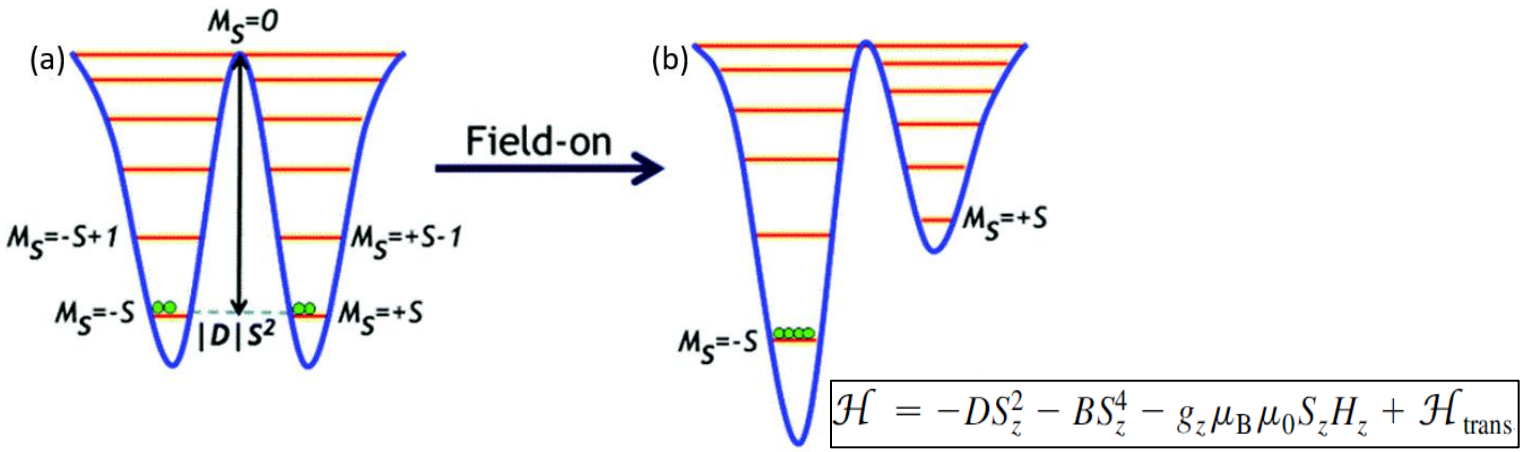

$$\mathcal{H} = -DS_z^2 - BS_z^4 - g_z\mu_B\mu_0 S_z H_z + \mathcal{H}_{\text{trans}}$$

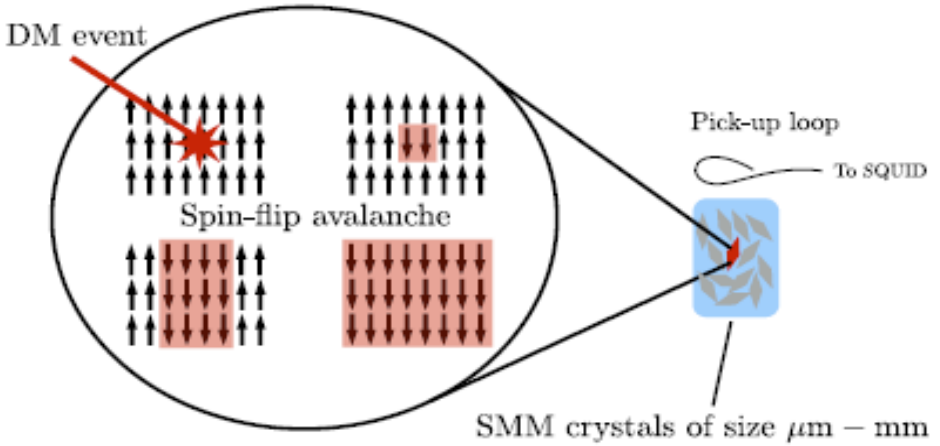

FIG. 1. DM detector concept based on magnetic deflagration in molecular nanomagnet crystals. A DM event that deposits energy in the form of heat ignites a spin-flip avalanche in the crystal which is detected by the change in magnetic flux through a pick-up loop.

[1] Bunting *et al. Phys. Rev. D* **95**, 095001 (2017)

Preliminary study using α particles [2,3]:
induced avalanches → **first evidence of Mn12 SMM as a sensor**

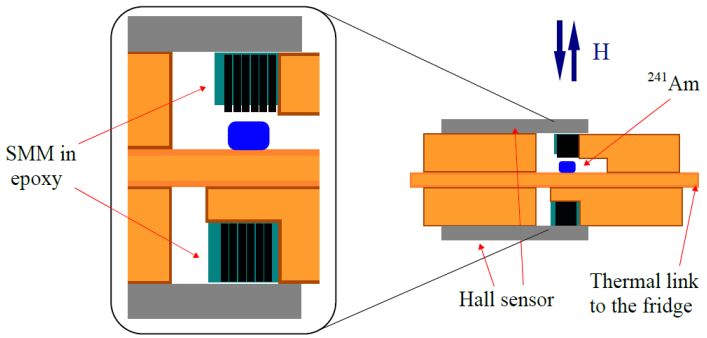

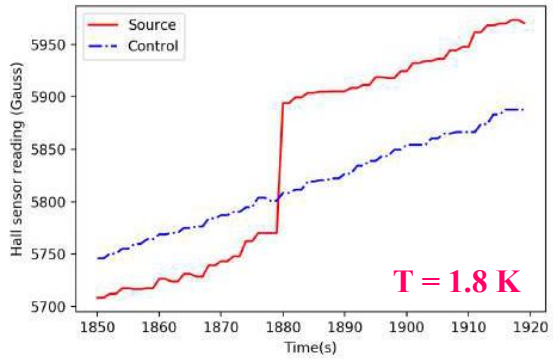

AIM OF THE NAMASSTE PROJECT:

- reproduce and optimize the conditions for α-induced magnetic avalanches (of potential interest for **up-scaling** in sensing volume ….);
- possibly extend to β and γ;
- **investigate other detection approaches.**

[2] Chen *et al.* arXiv:2002.09409v2; [3] Kohn, B. *et al.* arXiv:2508.02467

The INFN R&D NAMASSTE Project

NAMASSTE: NanoMagnets for quantum Sensing and Data Storage

The project (financed by INFN, CSNV) aims to design, synthesize, and characterize new molecular nanomagnets for two different applications:

- **single molecule magnets (SMMs)**, for **high-sensitivity** sensors, potentially suited for revealing dark matter hidden photon [1], …..;
- **single ion magnets (SIM)**, for **high-density** memory storage systems.

Focus of this talk

Novel combination of experimental techniques: **Magnetometry (SQUID), NMR, EPR, μ-SR**.

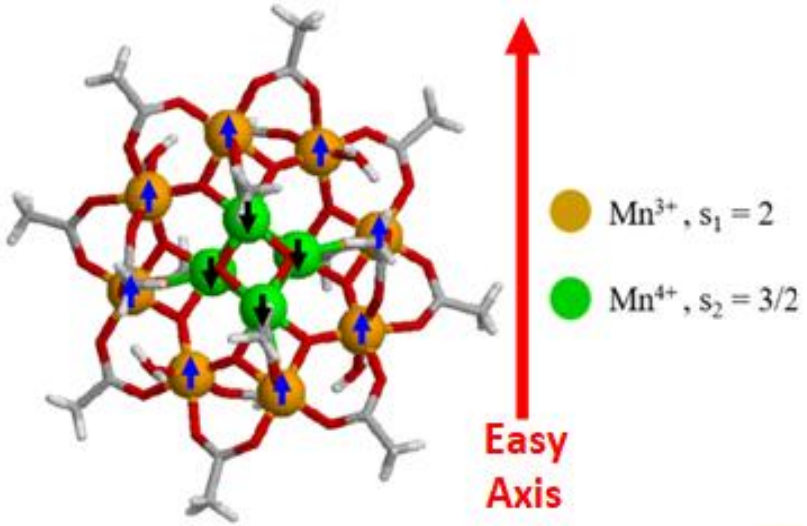

Mn_{12} SMM

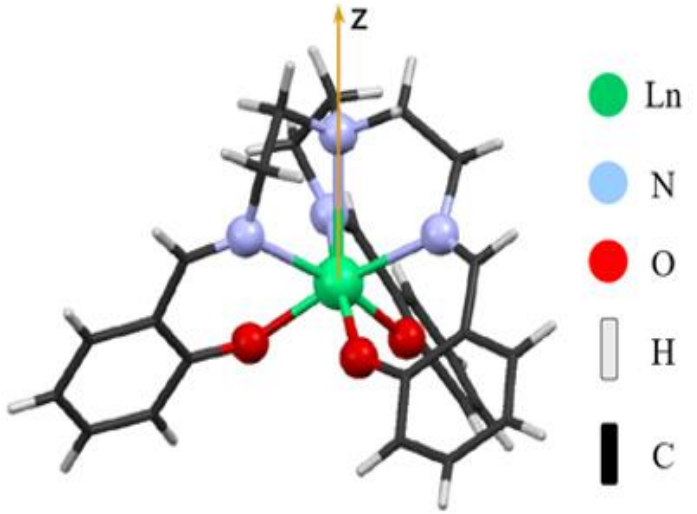

Ln-based SIM

[1] Bunting *et al. Phys. Rev. D* **95**, 095001 (2017)

NAMASSTE: Studies Related to Quantum Sensing

In NAMASSTE different techniques are used to study Mn_{12} in presence of **low activity** ionizing radiation sources

SQUID magnetometer

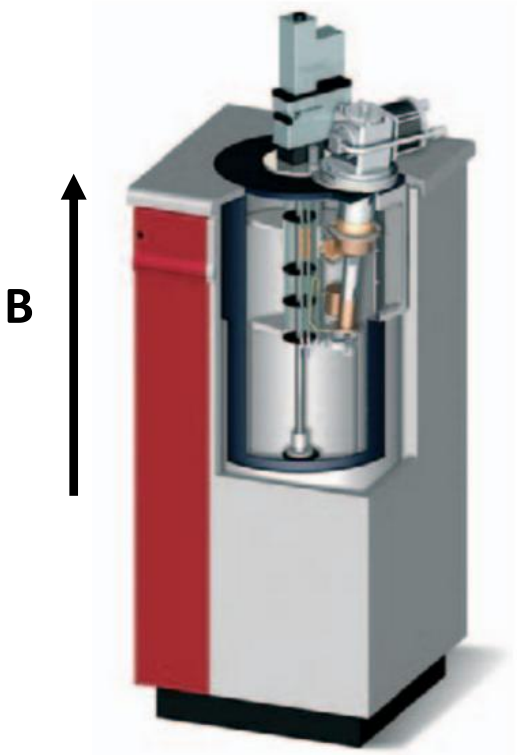

Measurement of the variation of the magnetization over the **entire volume** of the sensor: similar approach to the one reported in literature.

Nuclear Magnetic Resonance (NMR)

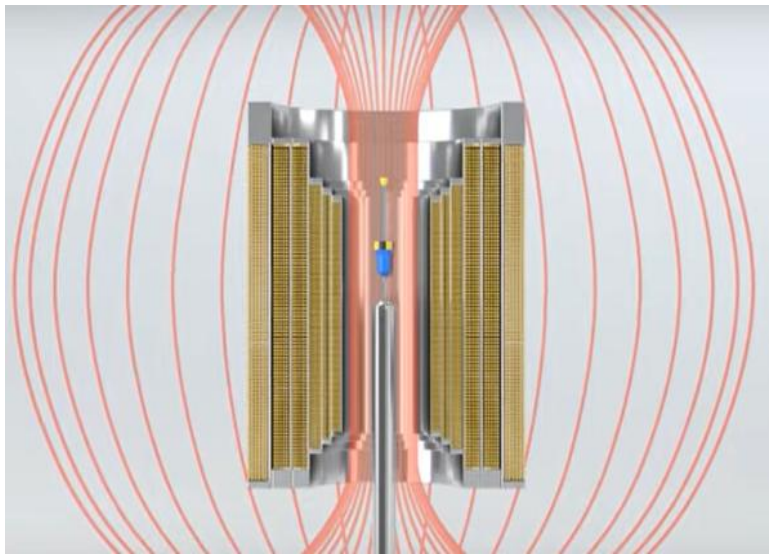

X-band Electron Paramagnetic Resonance (EPR)

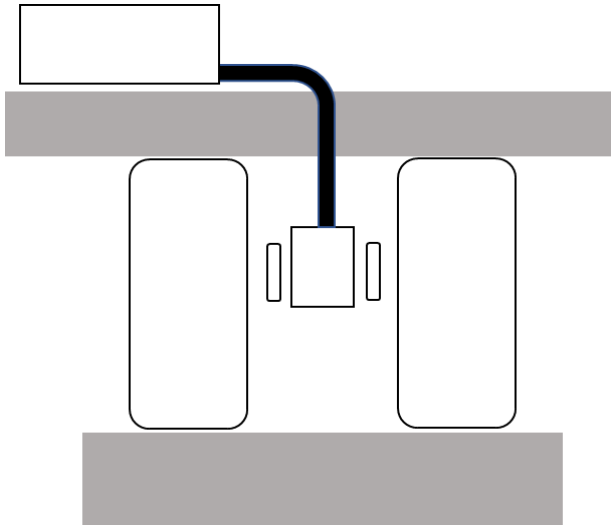

But Mn_{12} has S = 10
→ no intrinsic EPR signal ….

<u>Local probe techniques</u>: approaches based on the study of relaxation times, expected to be **more sensitive** than the ones based on magnetometry.

Radiation Sources for the NAMASSTE Experiment

Requirements: very low activity α, β, γ sources to be adapted to the small dimensions of the involved instruments

Made from electrodes used for special welding (tungsten with **2% Th)**, by precision machined cut to fit specific technical needs of the devices.

Measured surface activity:

- α (from prim./sec. decays) ~ 0.9 α /(mm^2 min)
- β (from sec. decays) ~ 30 times α activity
- γ (from sec. decays) ~ 225 times α activity

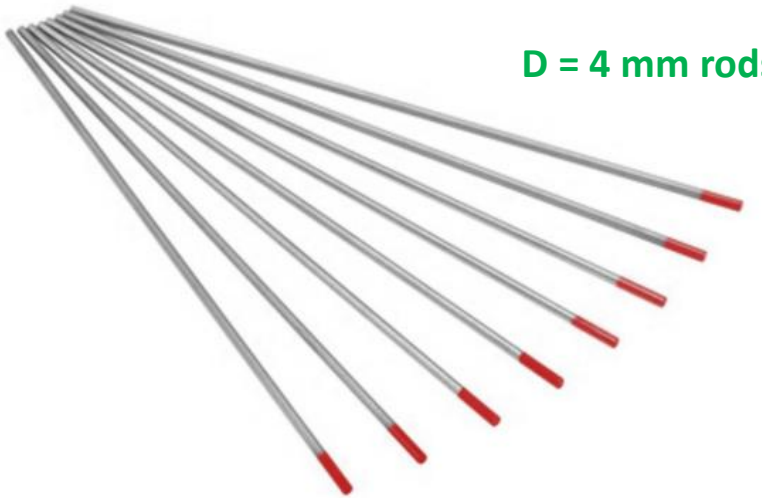

D = 4 mm rods

EPR-I: cylindrical geometry with small transversal cut

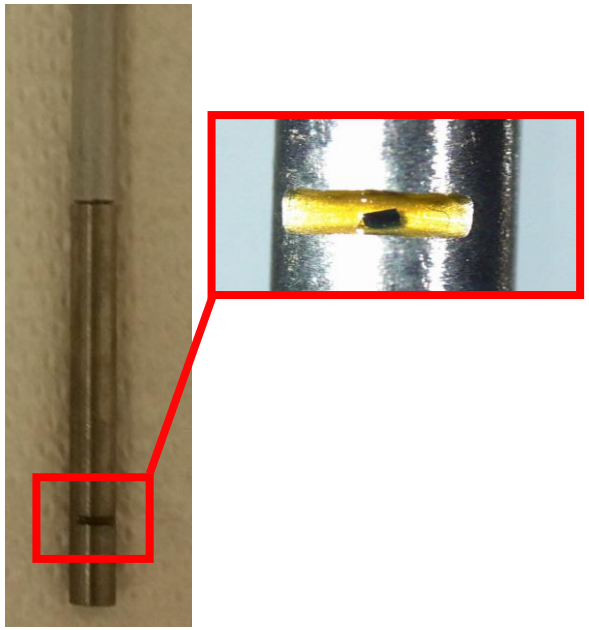

First approach, but:

- EPR signal very sensitive to position in cavity
- ~ 35 times reduction in EPR signal intensity w.r.t. using standard crystal sample holder

SQUID, NMR, EPR-II: semi-cylindrical geometry

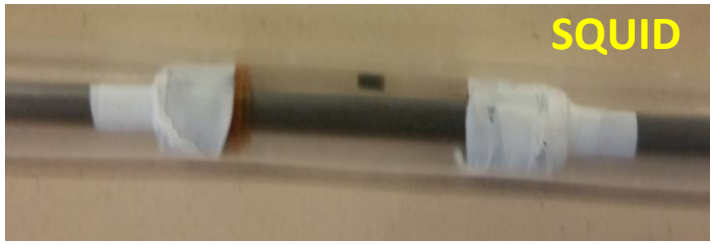

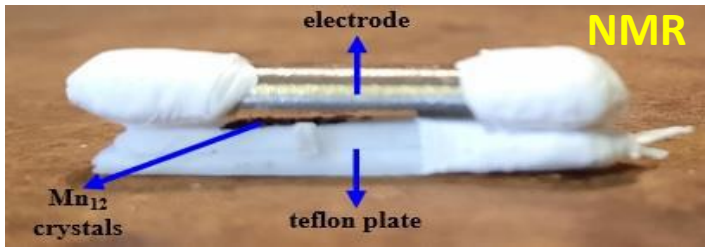

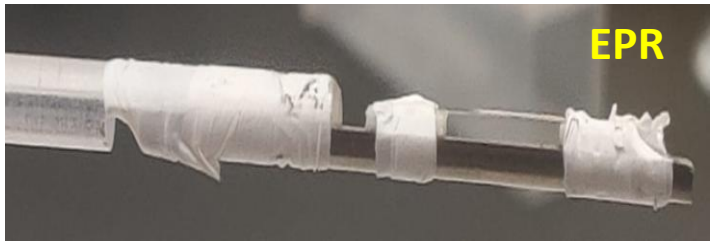

Availability of similar non-radioactive electrodes (w 2% La), to be used for "reference" measurements without particle radiation in the same experimental configuration.

SQUID Magnetometry Studies on Mn_{12}

Goal: reproduce the results reported in literature (induced avalanches) and identify the optimal conditions to obtain them.

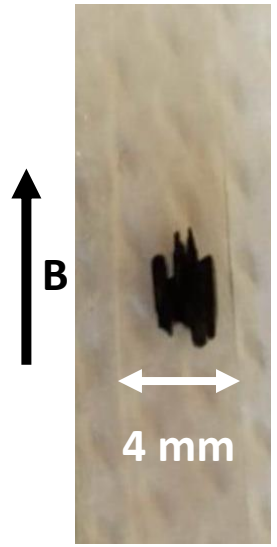

Crystals of Mn12 with the easy-axis // to the external magnetic field

Hysteresis curve w/w-out ionizing radiation source

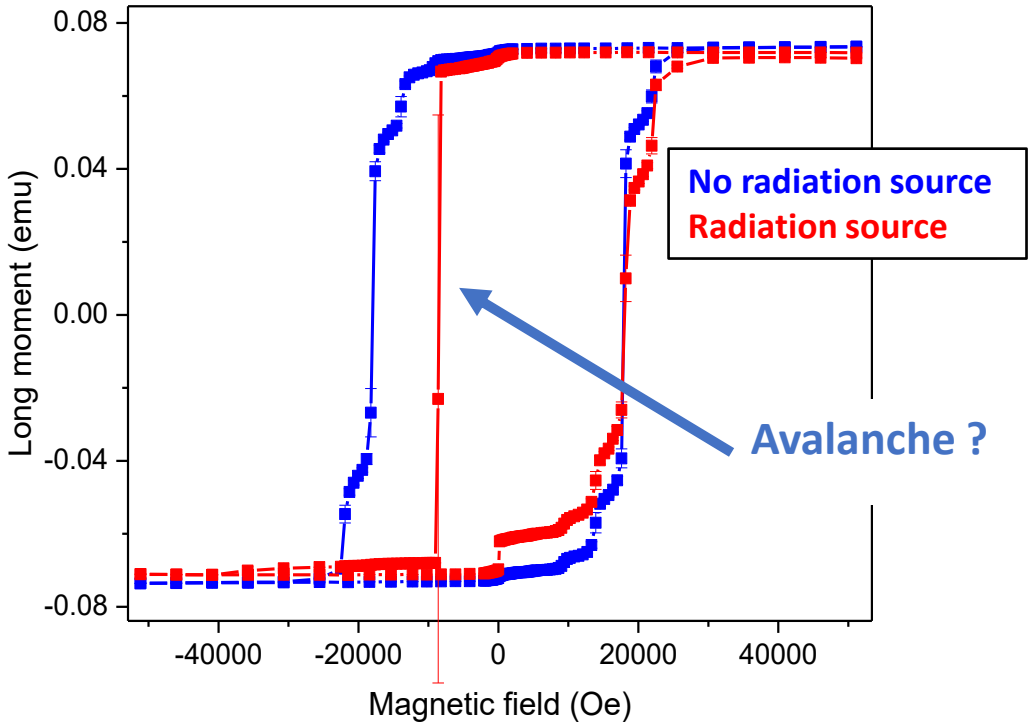

Relaxation curves with ionizing radiation source

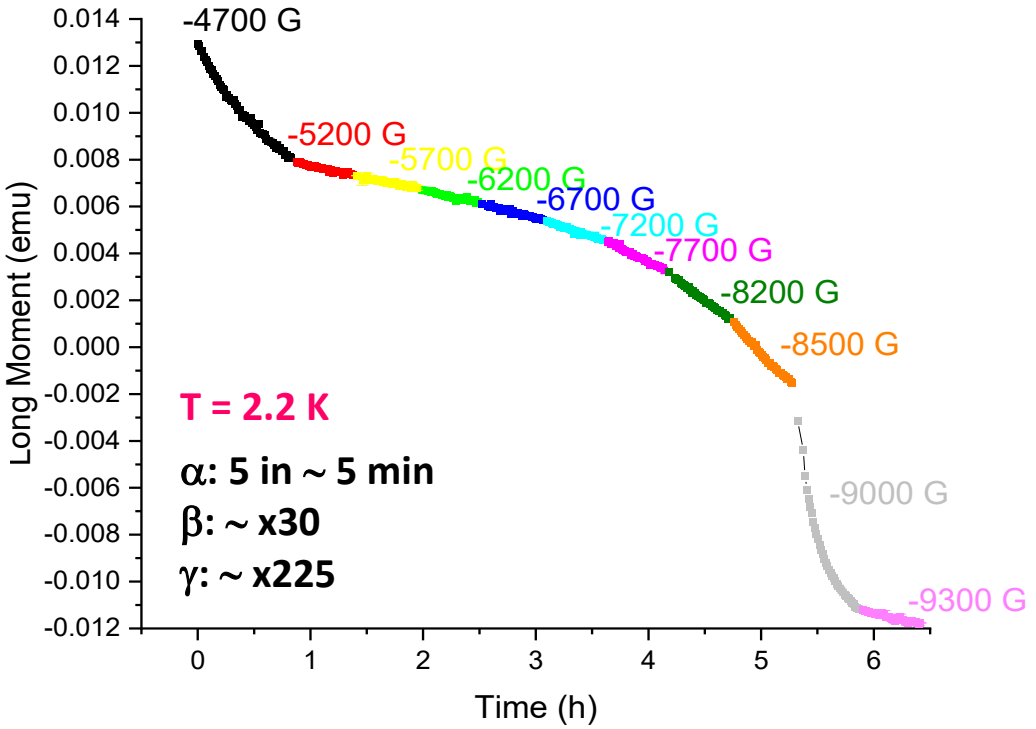

- **As expected, the hysteresis loops show 'jumps' at suitable B values due to quantum tunnelling effects.**
- **Abrupt reversal of magnetization, compatible with 'avalanche' effects, observed only in one case during hysteresis loops.**
- **Further extensive relaxation studies did not show induced avalanches.**

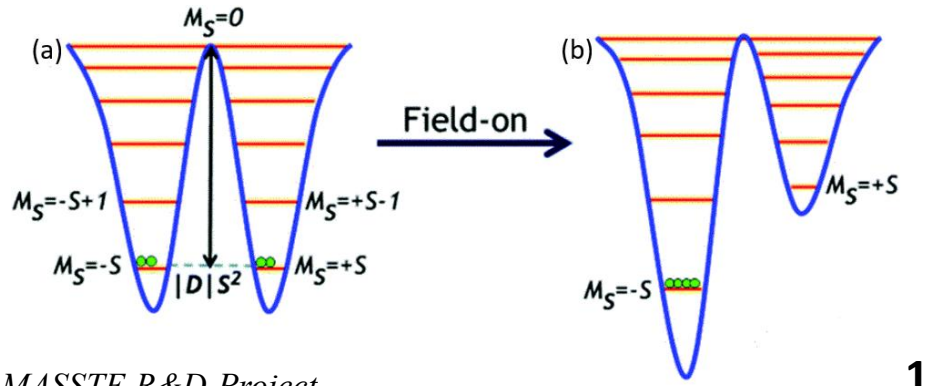

Electron Paramagnetic Resonance (EPR) Studies on Mn12

Goal: investigate the possibility to introduce a new detection approach, based on EPR techniques, by studying the behaviour of Mn12 crystals with/without irradiation.

EPR: absorption spectroscopy technique used to study chemical species with unpaired electrons; the details of EPR spectra depend on the electron interaction with the nearby environment (in our case, with the Mn12 magnetization).

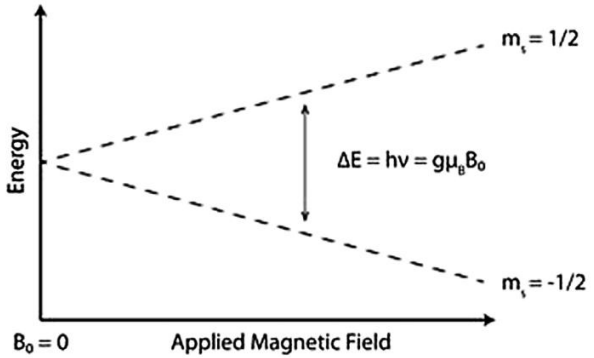

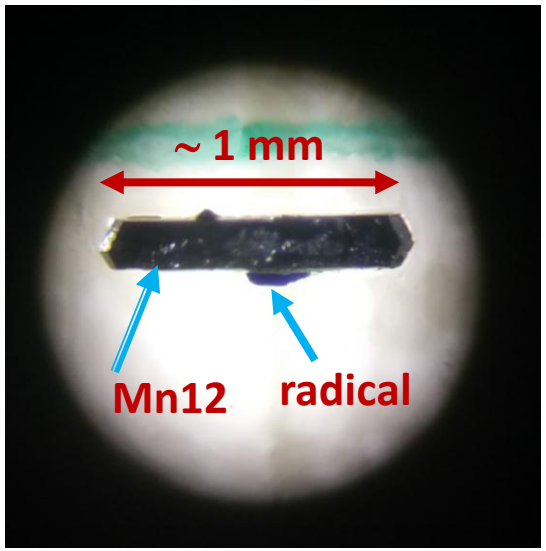

Adopted technique [1]:

- **Mn12 does not show an intrinsic EPR signal at the frequencies of the available device (X band).**
- **Then couple the Mn12 crystal to a radical crystal (specifically: NitPBAh, an organic radical), so to have an EPR signal sensitive to variations in Mn12 crystal magnetization.**

[1] Rakvin *et al.*, Jour. of Mag. Res., 165 (2003) 260-264

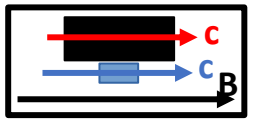

Chosen protocol (device driven):

- **Mn12+radical crystals cooled down to 3.9 K at B = 0 T.**
- **Then put B (// c-axis) around working value ~ 0.34 T.**
- **Get EPR signal (derivative of absorption spectrum) with measurements on short timescales (~ 1 ms) at a fixed B value.**
- **Check for induced perturbations in EPR spectra, by making stability studies in several runs of 400 10s-scans.**

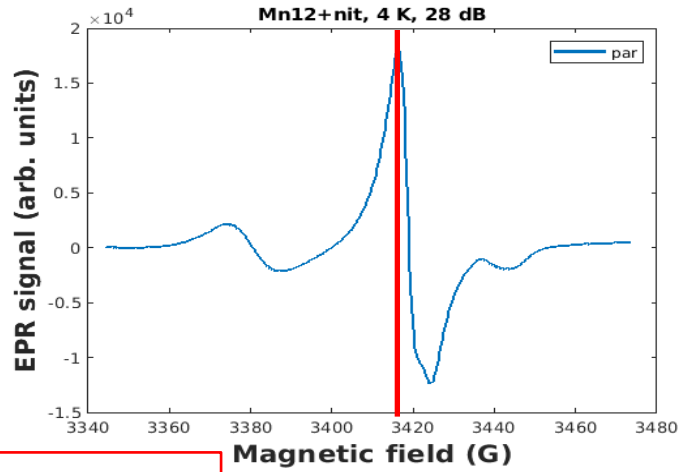

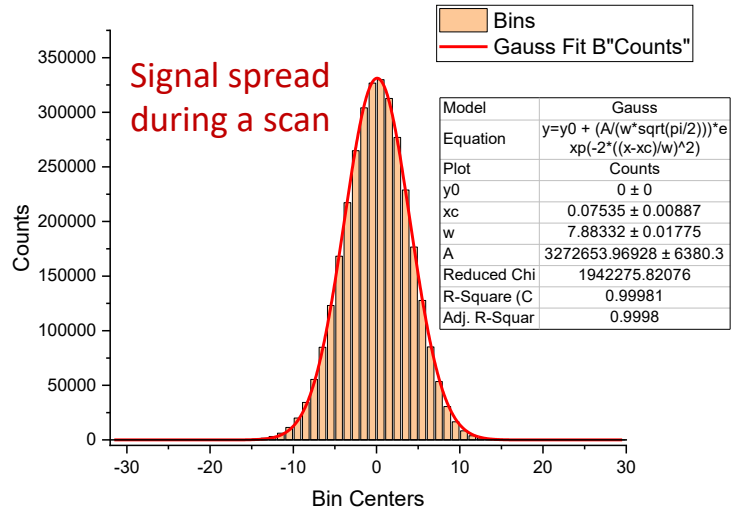

No indication of signal instability induced by ionizing radiation

NMR Studies on Mn_{12}

Goal: investigate the possibility to introduce a new detection approach, using NMR-based techniques, by studying the recovery time of Mn12 crystals with/without irradiation.

Adopted technique [1]:

- acquisition of the echo signal intensity height (related to the magnetization of the crystal) as a function of time;
- measurement of the recovery time τ of the magnetization from the related fit.

[1] Jang *et al.*, PRL 84 2977 (2000)

Chosen protocol:

- Mn12 crystal cooled down to ~ 2K at B = 0 T,
- then put at fixed B = 0.94 T (2rd crossing);
- start the measurements to follow the M recovery.

Relevant reduction in recovery time τ of M in presence of ionizing radiation

In order to establish a new detection method, based on studying perturbations on τ, further measurements and checks were performed to consolidate these results:

- at different B fields;
- similar studies with SQUID magnetometry.

^{1}H NMR echo height *h* vs time

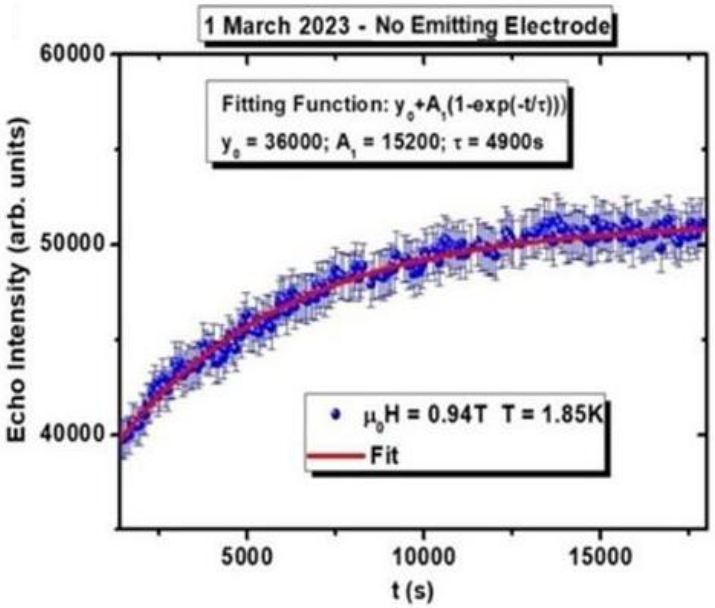

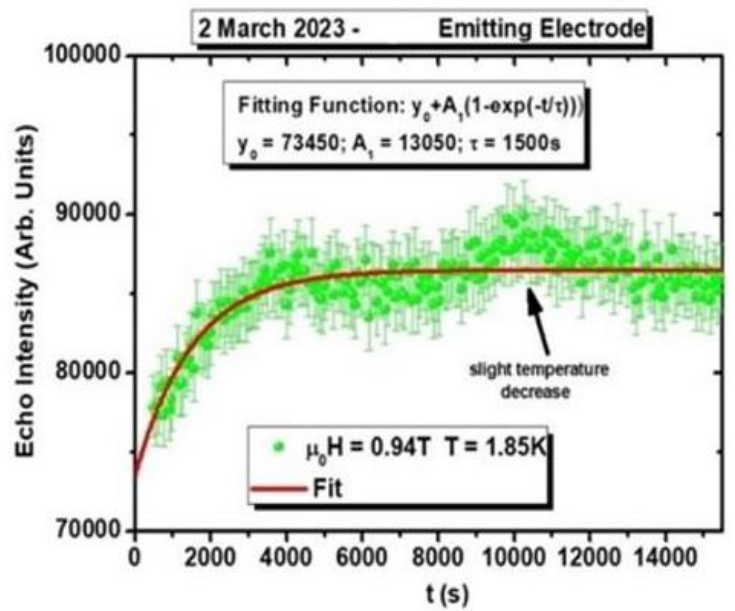

Run	τ (s), no radiation source	τ (s), radiation source
September 2022	10400	3500
March 2023	4900	1500

Mn_{12} SMMs as Sensors: Main NAMASSTE Results

Quantum sensing based on NMR and SQUID measurements: studies on recovery times

Normalized magnetization M vs t

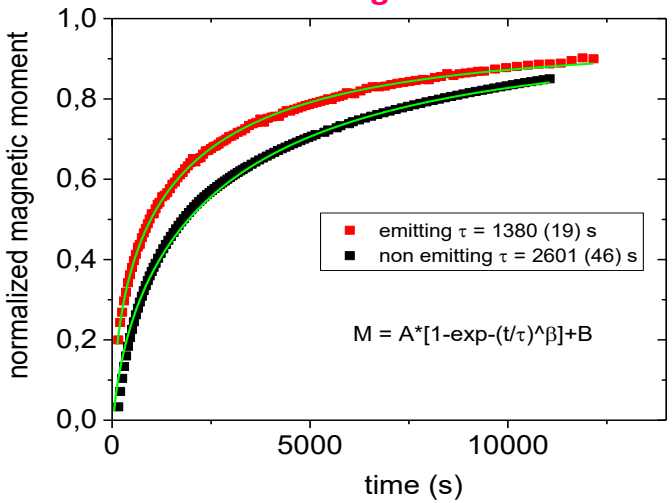

M recovery:
SQUID
NMR

^{1}H NMR echo height *h* vs t

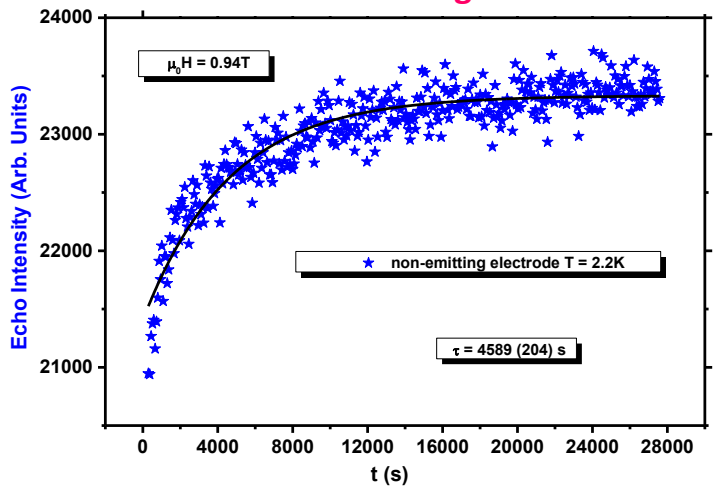

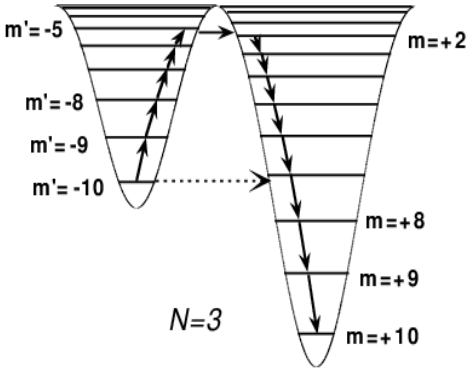

$$\mathcal{H} = -DS_z^2 - BS_z^4 - g_z\mu_B\mu_0 S_z H_z + \mathcal{H}_{trans}$$

Recovery time τ vs field, by SQUID

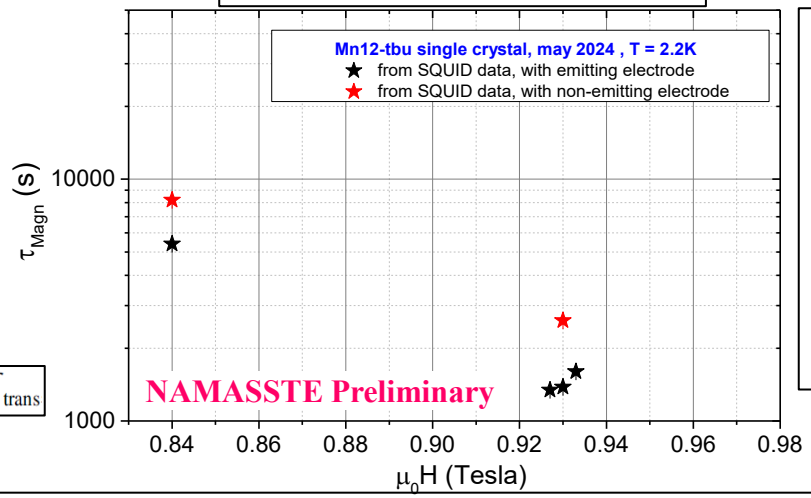

In SQUID and NMR experiments, a reduction in magnetization recovery time is observed due to impinging radiation (α, β, γ): **ionizing radiation induces perturbations in Mn12 spin dynamics**

Recovery time τ vs field, by NMR

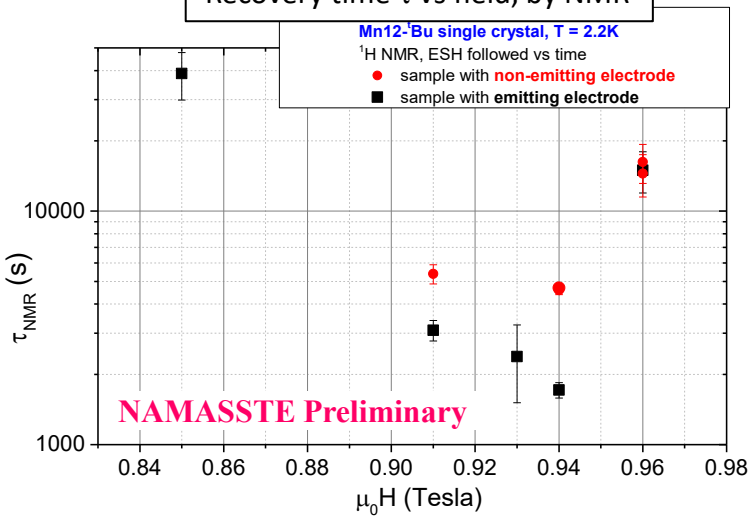

Exploring the potential of molecular nanomagnets as quantum sensors of radiation

(Submitted to Nat. Comm. Phys.)

Summary & Conclusions

- **In the search for New Physics (ex. DM) the development of devices based on Quantum Sensing for Particle Physics can play a key role.**

- **The NAMASSTE R&D project investigated the possibility to use SMMs as QS by studying Mn12 under the incidence of ionizing radiation with complementary techniques:**

  - SQUID magnetometry studies did not show induced "avalanche" effects;

  - EPR-based measurements did not show changes in the EPR absorption spectrum;

  - NMR- and SQUID-based studies showed a clear reduction in recovery time of M (i.e. perturbation in spin dynamics) induced by ionizing radiation:
  → introduction of a new detection technique, potentially opening to the use of SMMs as quantum sensors for particle detection.

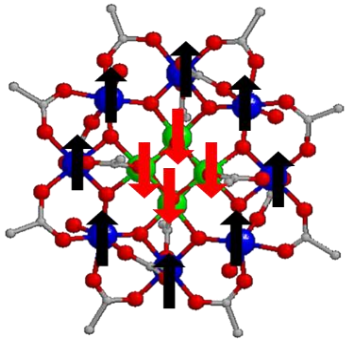

Mn_{12} core

- **Further studies ongoing to: get optimizations; set different sensing conditions; separate α, β, γ incidence; properly understand (also via theor. modelling) the SMM-radiation interaction.**

  → Next_NAMASSTE INFN R&D Project

The Dark Matter

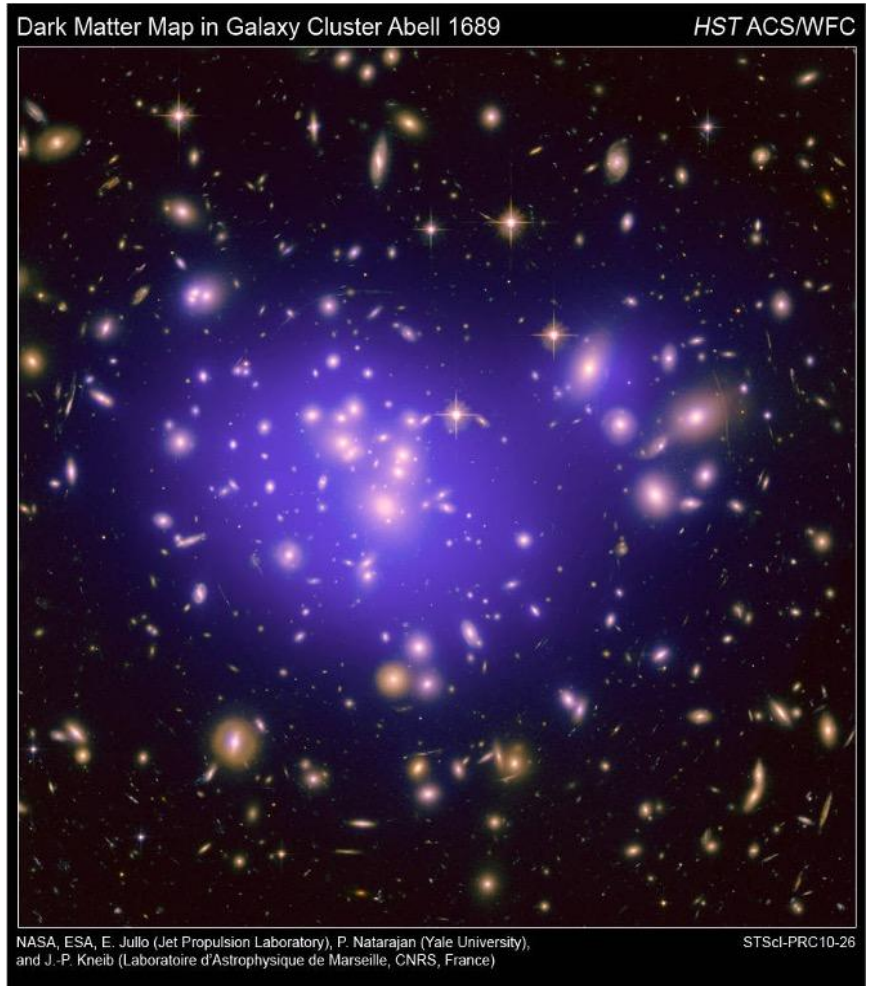

NASA's Hubble Space Telescope shows an immense cluster of galaxies located 2.2 billion light-years away. The cluster's gravitation warps light. Dark matter cannot be photographed, but its model distribution is shown in the blue overlay.

Cosmological and astronomical observations:

→ we are missing something …..

- **1933**: F. Zwicky observed that galaxies in the Coma cluster orbit much faster than their combined mass can explain; he postulated the existence of a new form of invisible matter, which he named "***Dark Matter***".

- **1970**: V. Rubin and W.K. Ford discovered that the rotational curves of galaxies are **flat**

$$\frac{GMm}{r^2} = m\frac{v^2}{r} \Rightarrow v = \sqrt{\frac{GM(r)}{r}}$$

$$v = const. \Rightarrow M(r) \sim r$$

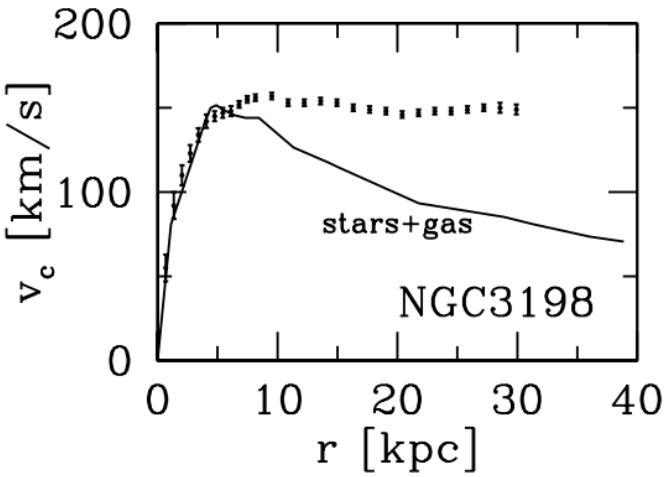

→ If modifications on General Relativity are excluded, the Dark Matter overcomes the ordinary matter in galaxies, even outside their core ….

CERN Quantum Technology Initiative

- Assess the **areas of potential quantum advantage** in HEP applications (QML, classification, anomaly detection, tracking)
- Develop **common libraries of algorithms, methods, tools**; benchmark as technology evolves
- Collaborate to the development of shared, **hybrid classic-quantum infrastructures**

Computing & Algorithms

- Identify and develop techniques for **quantum simulation** in collider physics, QCD, cosmology within and beyond the SM
- Co-develop quantum computing and sensing approaches by providing **theoretical foundations** to the identifications of the areas of interest

Simulation & Theory

- Develop and promote **expertise in quantum sensing** in low- and high-energy physics applications
- Develop quantum sensing approaches with emphasis on **low-energy particle physics measurements**
- Assess **novel technologies and materials** for HEP applications

Sensing, Metrology & Materials

- **Co-develop CERN technologies relevant to quantum infrastructures** (time synch, frequency distribution, lasers)
- Contribute to the **deployment and validation of quantum infrastructures**
- Assess requirements and **impact of quantum communication on computing applications** (security, privacy)

Communications & Networks

https://quantum.cern/

Some Details on Mn_{12} SMM (I)

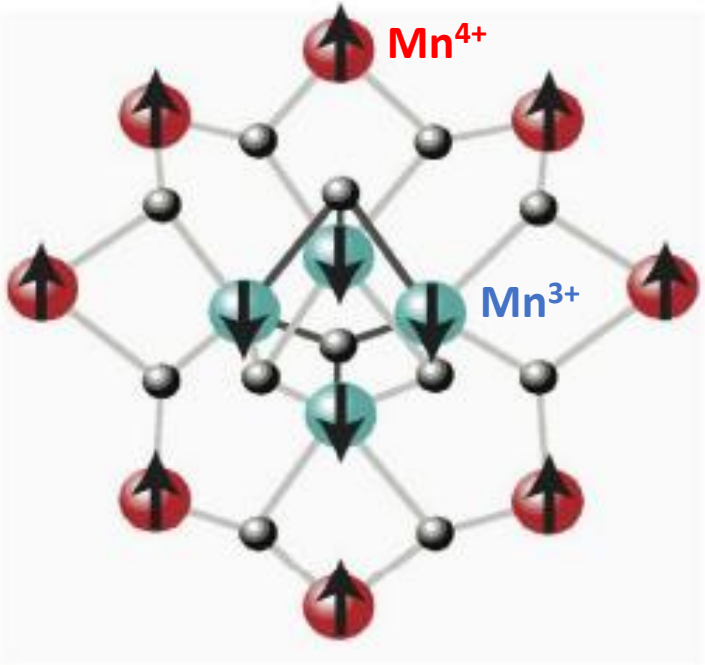

[5] arXiv:1001.4194v2

The magnetic core of Mn12-ac has 4 Mn^{3+} (S = 3/2) ions in a central tetrahedron surrounded by 8 Mn^{4+} (S = 2) ions. The ions are coupled by superexchange through oxygen bridges with the net result that the four inner and eight outer ions spins point in opposite directions, yielding a total spin S = 10. The magnetic core is surrounded by acetate ligands, which serve to isolate each core from its neighbors and the molecules crystallize into a body-centered tetragonal lattice. While there are very weak exchange interactions between molecules, the exchange between ions within the magnetic core is very strong, resulting in a rigid spin 10 object that has no internal degrees of freedom at low temperatures.

Mn — O — Mn

Superexchange in MnO:
on each side the (O-Mn) electron couple has spin = 0 → the Mn on the 2 sides have opposite spin

Superexchange interaction through oxygen bridges →

- **ferromagnetic coupling among the 4 inner Mn^{3+} and 8 outer Mn^{4+} ions.**
- **antiferromagnetic coupling among inner Mn^{3+} and outer Mn^{4+} ions.**

Some Details on Mn_{12} SMM (II)

Mn_{12} Spin Hamiltonian (in absence of an "external perturbation")

$$H = H_0 + H_c$$

H_0 is the "internal Hamiltonian": $H_0 \approx - DS_z^2 - AS_z^4 + H'$ (H': non axial contribution)

$D = 0.548$ K, $A = 1.173 \cdot 10^{-3}$ K

H_C is the "control Hamiltonian": $H_c = - g_z \mu_B S_z B_Z$ (Zeeman energy due to z-axis oriented magnetic field)

$g_z = 1.94$

H' contains non axial (tunnelling) terms: $H' \approx E(S_x^2 - S_y^2) + (C/2)(S_+^4 + S_-^4) - g\mu_B S_x H_x + \ldots$

H_X due to any possible "internal" field

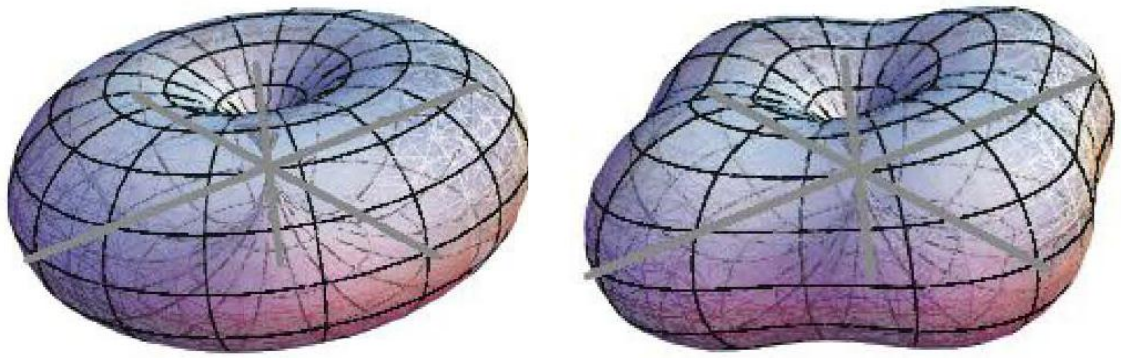

Left: spherical polar plots of energy as a function of orientation for a classical spin with uniaxial anisotropy. Right: same as above, with additional fourth-order transverse anisotropy [1].

[1] Friedman and Sarachik, *Ann. Rev. Cond. Matt. Phys.* ***1,*** *109* (2010)

Some Details on Mn_{12} SMM (III)

Control Hamiltonian $H_c = - g_z \mu_B S_z H_Z$

obtained with a magnetic field H oriented along the main crystal c-axis (easy axis)

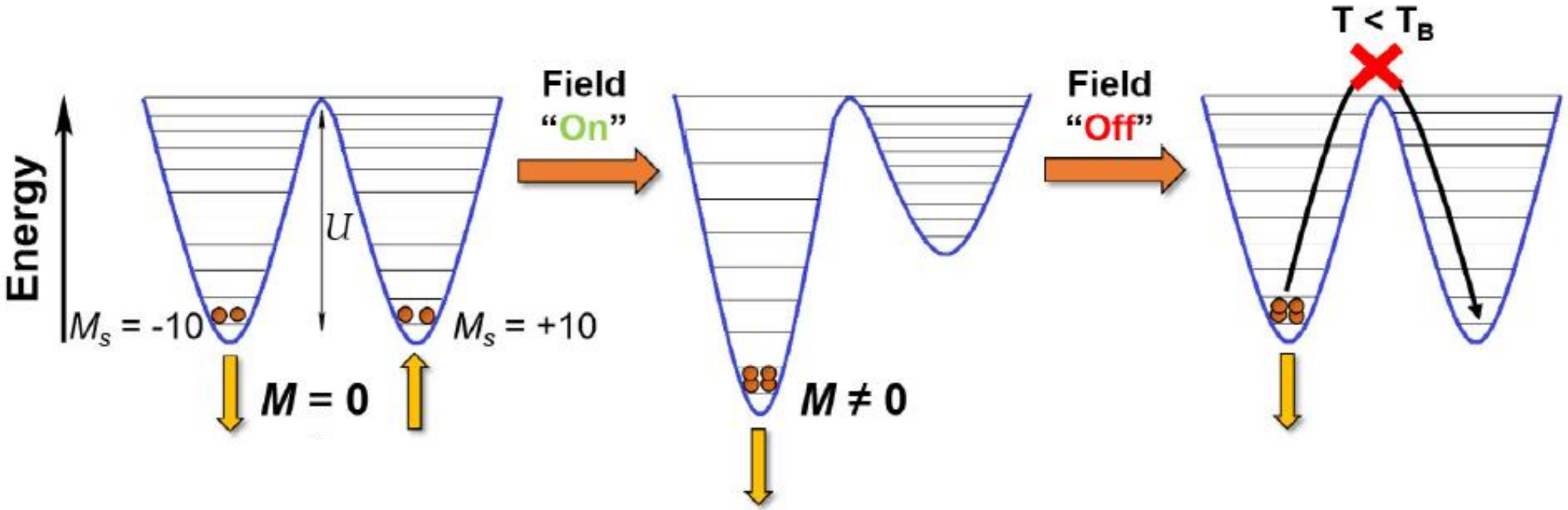

Some Details on Mn_{12} SMM (IV)

$H = H_0 = - DS_z^2 - AS_z^4 + H'$ $\quad$ $H \approx - DS_z^2 + H' + H_C$ $\quad$ $H = - DS_z^2 - AS_z^4 + H' + H_C$

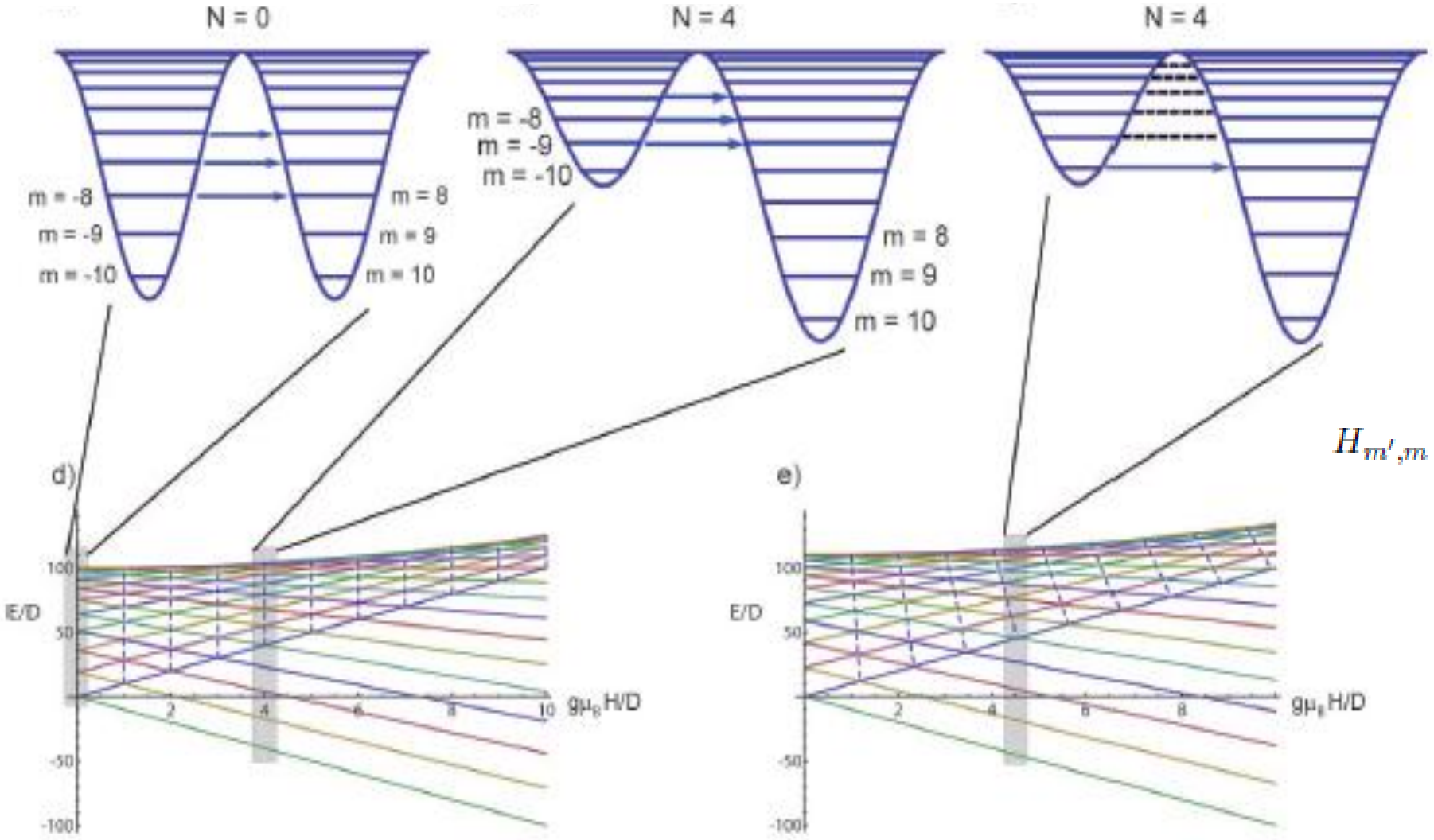

Energy levels "align" if:

$$H_N = ND/g_z\mu_B \qquad \text{for A = 0}$$

$$H_{m',m} = \frac{D(m'+m)}{g_z\mu_B}\left[1 + \frac{A}{D}(m'^2 + m^2)\right]$$

for A ≠ 0 (N = m' + m)

Macroscopic Quantum Effects in Hysteresis Loops

Hysteresis loops on Mn12 (no α) at different T

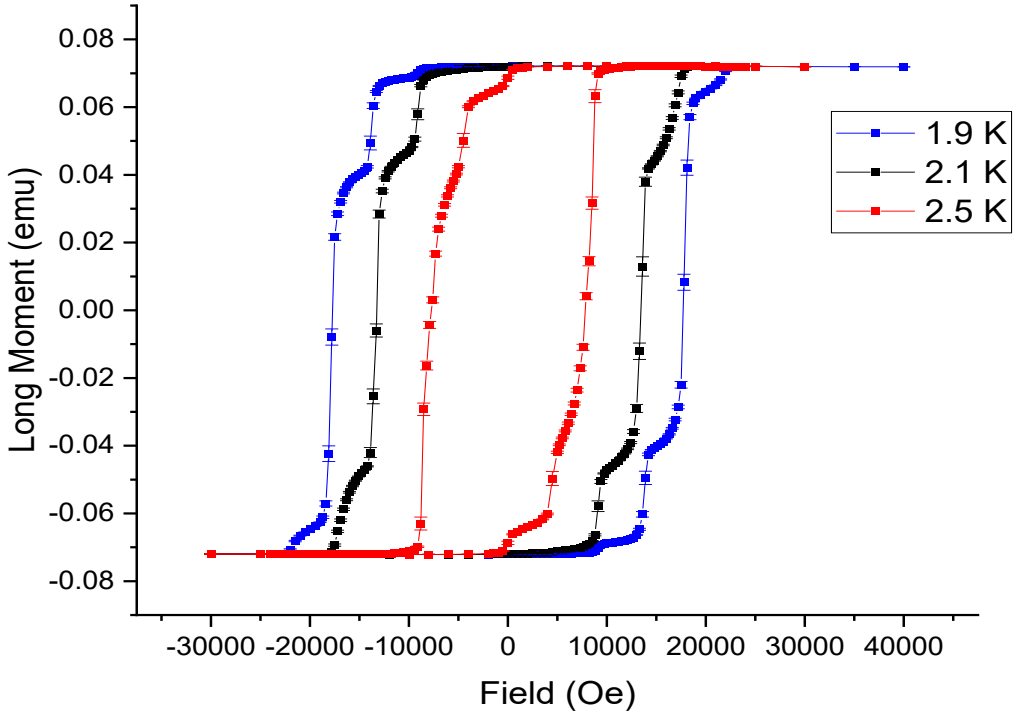

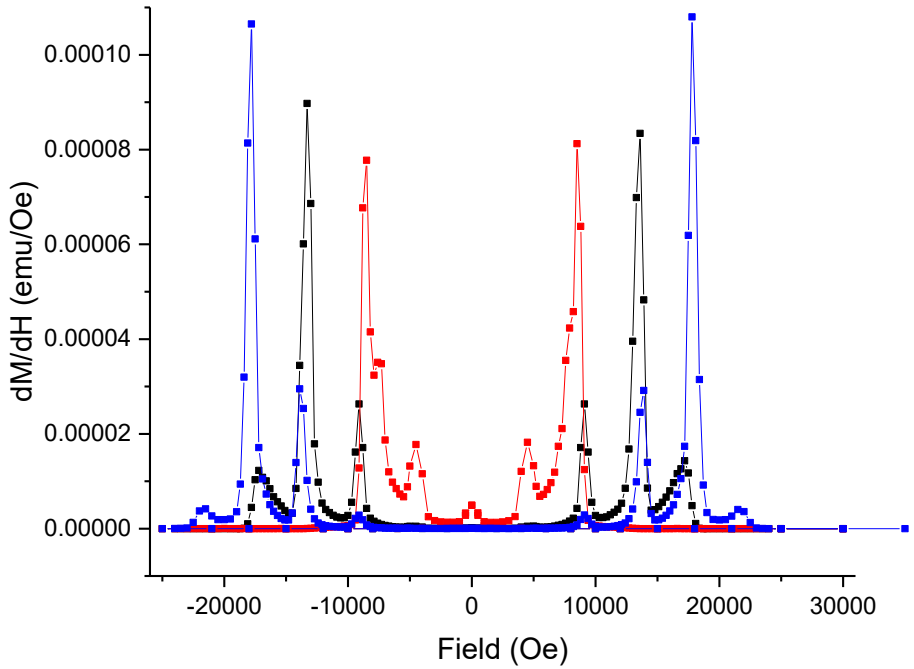

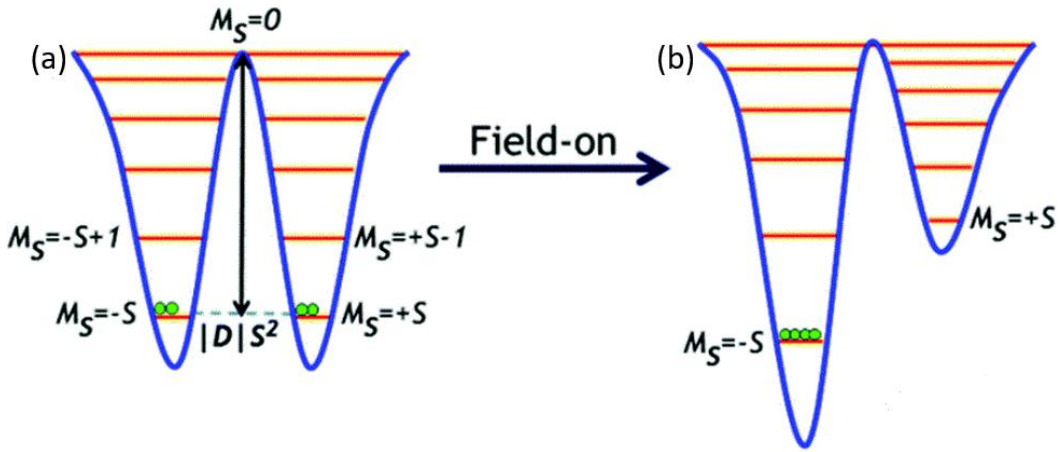

1° jump = 0 Oe
2° jump = 5000 Oe
3° jump = 9100 Oe
4° jump = 13900 Oe
5° jump = 17800 Oe
6° jump = 21500 Oe

Strong Dependence of Relaxation Time τ on *T* and B

QTM Direct Raman Orbach

$$\frac{1}{\tau} = \frac{A_1}{1+A_2B^2} + CB^2T + DT^n + \frac{1}{\tau_0}\exp(-\tilde{U}(B)/kT)$$

$$\tilde{U}(B) = U - \frac{1}{2}\Delta E_{\mathrm{Zee}}, \text{ with } \Delta E_{\mathrm{Zee}} = 2\mu_B g_J JB$$

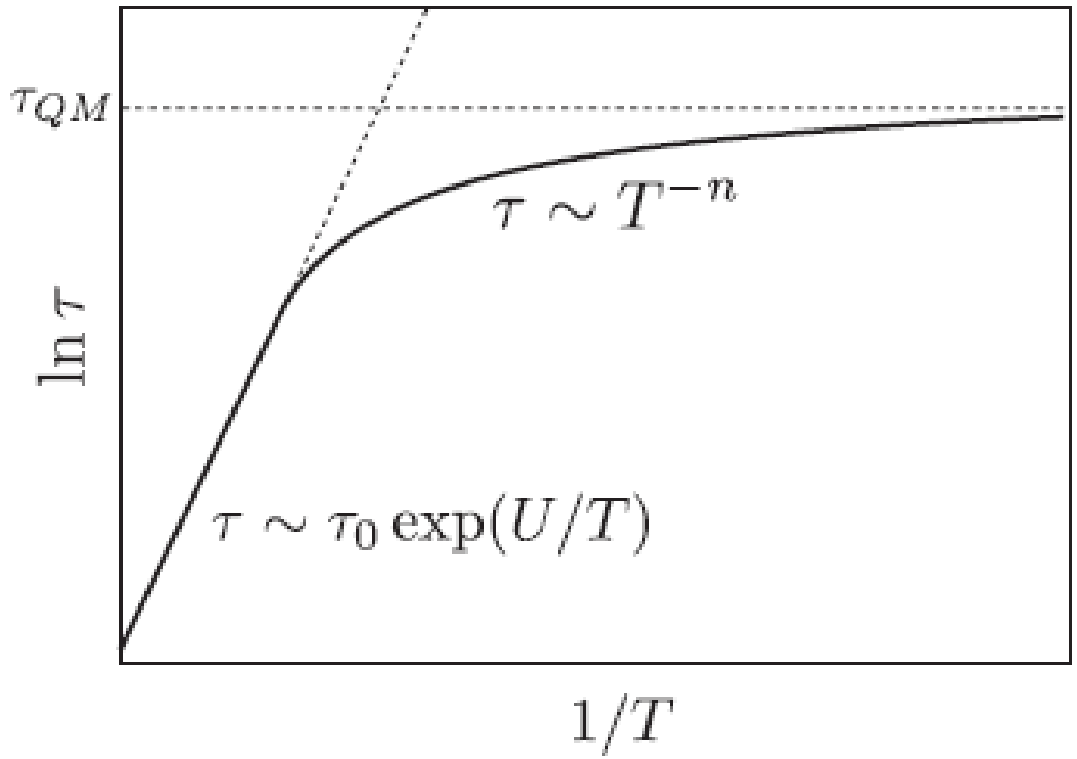

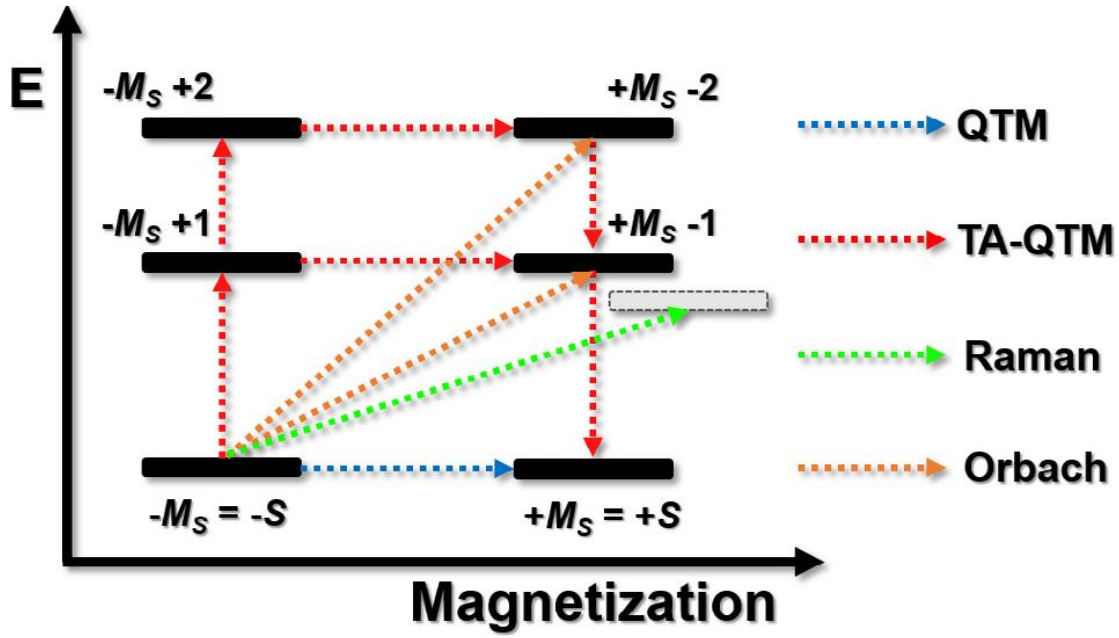

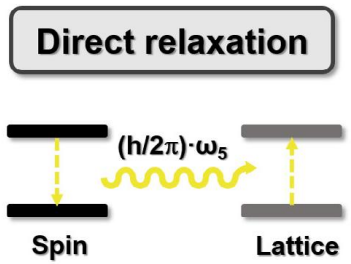

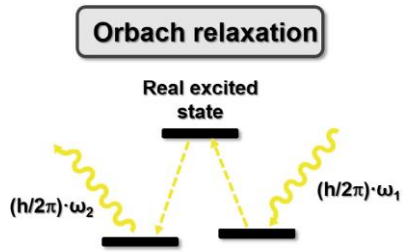

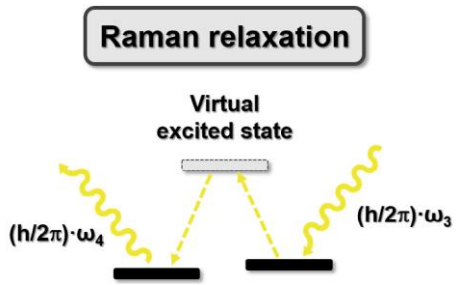

Modelling of Radiation-Induced Perturbation in M Dynamics

The simulation considers: the Mn_{12} SMM spin Hamiltonian with two axial terms and one term for the tunnelling; a standard model for the spin-phonon coupling; master equation for the relaxation.

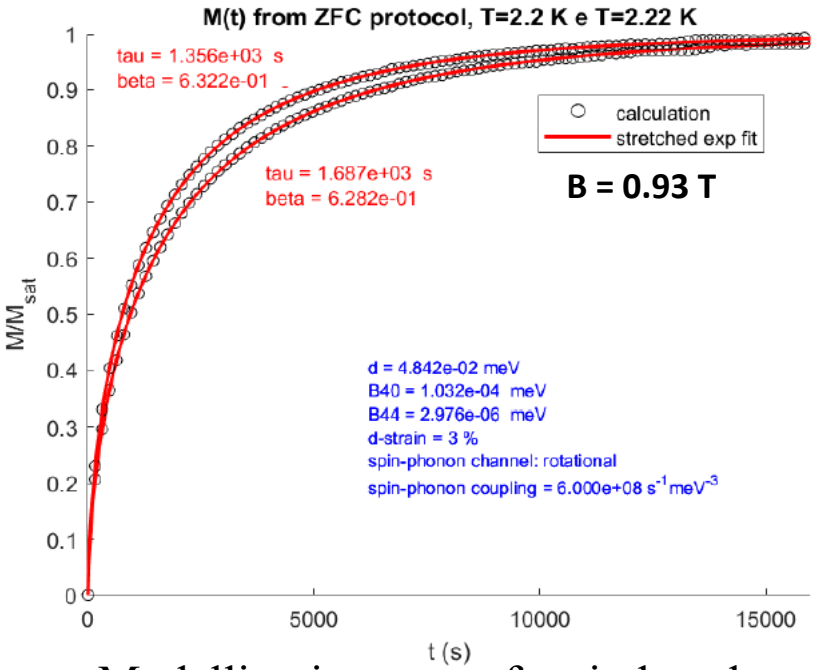

Modelling in terms of an induced (0.02K) global increase in temperature

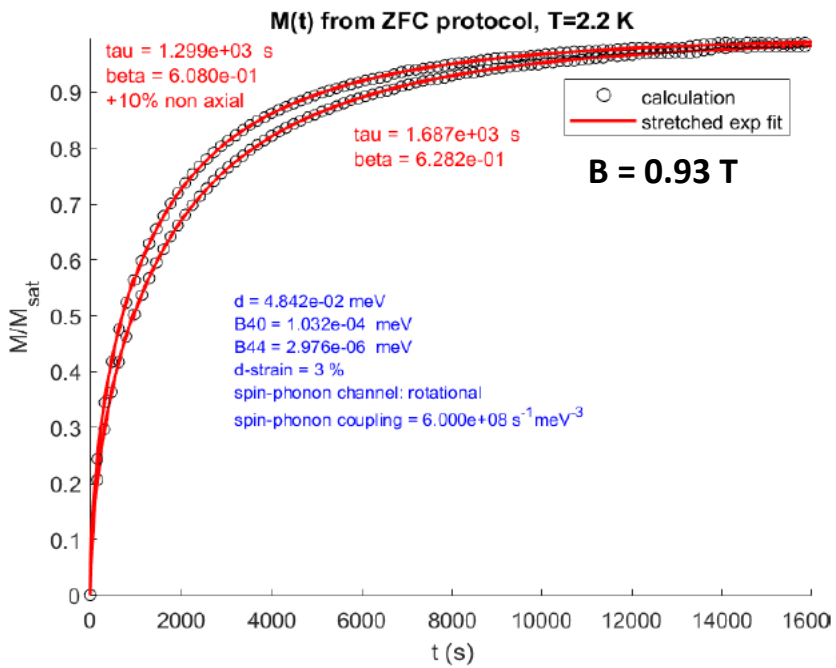

Modelling in terms of an induced increase in tunnelling mechanism

$$H = -D\hat{S}_z^{\,2} - C\hat{S}_z^{\,4} + B_4^4 \frac{1}{2}(\hat{S}_+^4 + \hat{S}_-^4) - g\mu_B B\hat{S}_z$$

B (T)	Configuration	τ (s)	β
0.84	Standard	8584	0.9017
	Increase in T	6808	0.8908
	Increase in B_4^4	6544	0.8928
0.93	Standard	1687	0.6282
	Increase in T	1356	0.6322
	Increase in B_4^4	1299	0.6080

Simulation of SQUID Setup with the PHITS Code

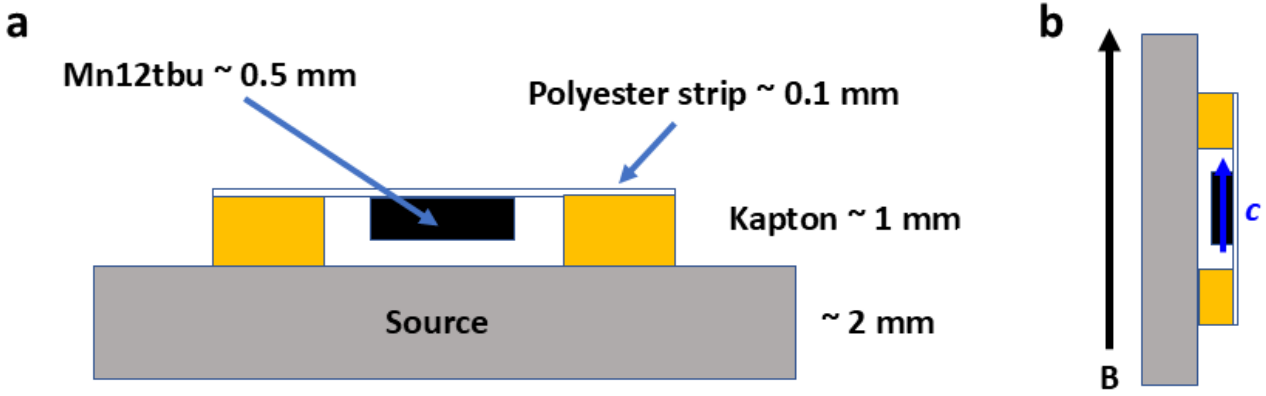

γ emission spectrum

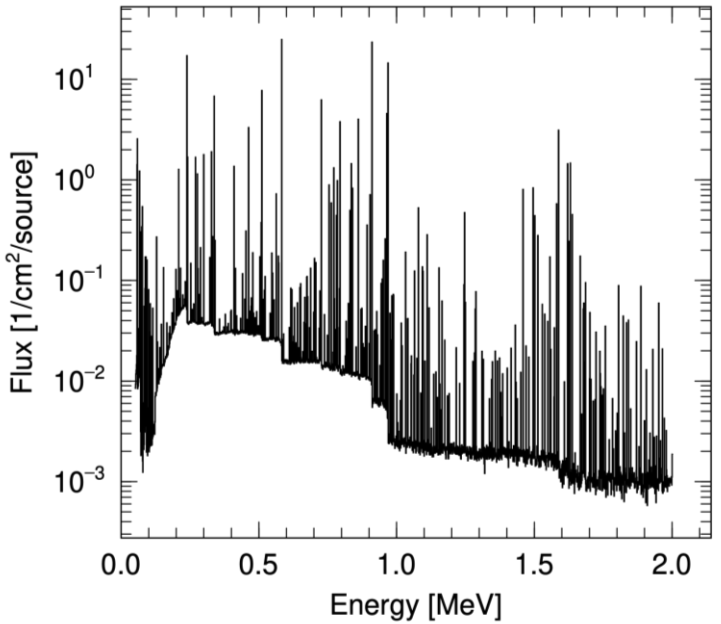

Table 3. Characterization of ionizing radiations emitted from radioactive sources. Top and middle rows: measured surface radiation fluxes and energy range. Bottom row: simulated average radiation dose per particle in the crystal volume.

	α emission	β emission	γ emission
Surface flux (particles/mm^2·min)	~ 0.9	~ 26	~ 204
Energy range	(0 - 9.8) MeV	(0 – 834) keV	(59 – 1954) keV
Average dose (Gy/particle)	$(2.2 \pm 0.3) \times 10^{-8}$	negligible	$(9.0 \pm 0.2) \times 10^{-10}$

The absorbed dose in the crystal is mostly driven by γ radiation:

- photons release a dose about a factor of 10 greater than the one due to α particles, while the β release results negligible;
- mainly low energy photons (E < 100 keV) interact by photoelectric effect, while higher energy photons rarely interact (44% of the photons in this E range, representing about 40% of the total, are absorbed, while by far more than 99% of the photons in the higher energy range cross the crystal without interacting);
- in correspondence of this absorbed dose, a *T* increase is estimated well below 10^{-4} K over a typical measurement of 4 h

→ we can reasonably be confident that there is not substantial global thermal effect, due to impinging radiation, which could account for the observed effect …..